Food and Chemical Toxicology 118 (2018) 608–625

Contents lists available at ScienceDirect

Food and Chemical Toxicology

journal homepage: www.elsevier.com/locate/foodchemtox

Subchronic dietary exposure to ethoxyquin dimer induces microvesicular steatosis in male BALB/c mice

Annette Bernhard[a], Josef D. Rasinger[a], Helene Wisløff[b], Øyvor Kolbjørnsen[b], Lene Secher Myrmel[a], Marc H.G. Berntssen[a], Anne-Katrine Lundebye[a], Robin Ørnsrud[a,*], Lise Madsen[a,c]

[a] Institute of Marine Research, P.O. BOX 1870 Nordnes, N-5817 Bergen, Norway
[b] Pathology Section, Norwegian Veterinary Institute, P.O. BOX 750 Sentrum, N-0106 Oslo, Norway
[c] Department of Biology, University of Copenhagen, Universitetsparken 13, DK-2100 Copenhagen, Denmark

ARTICLE INFO

Keywords:
Food safety
Feed additives
Ethoxyquin
Hepatotoxicity
Benchmark dose
Multi-level omics

ABSTRACT

The use of the synthetic antioxidant ethoxyquin (6-ethoxy-2,2,4-trimethyl-1,2-dihydroquinoline; EQ) in animal feed results in the presence of EQ residues and metabolites, including the EQ dimer (1,8′-bi(6-ethoxy-2,2,4-trimethyl-1,2-dihydroquinoline); EQDM) in animal food products. To investigate the toxicity and dose-response of dietary exposure to EQDM, male BALB/c mice were exposed to one of six dietary doses of EQDM, ranging from 0.015 to 518 mg/kg body weight/day for 90 days. Doses above 10 mg/kg body weight/day affected whole body lipid metabolism resulting in increased liver weights and decreased adipose tissue mass. Metabolomic screening of livers revealed alterations indicating incomplete fatty acid β-oxidation and hepatic oxidative stress. Histopathological evaluation and biochemical analyses of the liver confirmed the development of microvesicular steatosis and activation of the glutathione system. Hepatic protein profiling and pathway analyses suggested that EQDM-induced responses are mediated through activation of CAR/PXR nuclear receptors and induction of a NRF2-mediated oxidative stress response. Based on the development of microvesicular steatosis as the critical endpoint, a Reference Point for dietary EQDM exposure was established at 1.1 mg/kg body weight/day ($BMDL_{10}$) from benchmark dose modelling. Applying an uncertainty factor of 200, an Acceptable Daily Intake of 0.006 mg EQDM/kg body weight was proposed.

1. Introduction

Ethoxyquin (6-ethoxy-2,2,4-trimethyl-1,2-dihydroquinoline; EQ) is a synthetic antioxidant, which has been widely used in animal feed for pets, livestock and farmed fish as a technological additive to protect against lipid peroxidation. EQ is not authorized as a food additive in the European Union. The presence of EQ in feed for livestock and farmed fish results in residues of EQ and its metabolites in edible tissue of animal origin (Bohne et al., 2008; Lundebye et al., 2010; Hobson-Frohock, 1982; Wang et al., 2015; He and Ackman, 2000). Thus, humans can be exposed to EQ residues and metabolites through their diet.

An Acceptable Daily Intake (ADI) of 0.005 mg/kg body weight was established for EQ and several metabolites by the Joint Food and Agricultural Organization and World Health Organization Meeting on Pesticide Residues (JMPR) based on clinical signs observed in dogs exposed to 2.5 mg EQ/kg body weight in feed (JMPR, 1998). However, this ADI was not confirmed by the European Food Safety Authority (EFSA) in its review of the Maximum Residue Levels (MRLs) for EQ as a pesticide (EFSA, 2013).

In addition to the parent compound, the ADI for EQ set by the JMPR also included the intake of three metabolites found in plants, namely methylethoxyquin, dihydroethoxyquin and dehydrodemethylethoxyquin (Gupta and Boobis, 2005; EFSA, 2013). In salmon, EQ from fish feed is rapidly metabolized (Skaare and Roald, 1977) to at least 14

Abbreviations: ADI, Acceptable Daily Intake; AIC, Akaike Information Criterion; ALT, Alanine transferase; AST, Aspartate transferase; BMD, Benchmark dose; BMDL, Lower bound benchmark dose; BMDU, Upper bound benchmark dose; BMR, Benchmark response; CAR, Constitutive androstane receptor; EFSA, European Food Safety Authority; EQ, Ethoxyquin; EQDM, Ethoxyquin dimer; FFA, Free fatty acid; GSH, Reduced glutathione; GSSG, Oxidized glutathione; IPA, Ingenuity pathway analysis; KEAP1, Kelch-like ECH-associated protein 1; NOAEL, No-observed-adverse-effect-level; NRF2, Nuclear factor erythroid 2-related factor 2; PXR, Pregnane-X-Receptor; ROS, Reactive oxygen species; TAG, Triacylglycerides; TBARS, Thiobarbituric acid reactive substances

* Corresponding author.
E-mail address: robin.ornsrud@hi.no (R. Ørnsrud).

https://doi.org/10.1016/j.fct.2018.06.005
Received 5 March 2018; Received in revised form 11 May 2018; Accepted 4 June 2018
Available online 05 June 2018

transformation products (Bohne et al., 2007a). Three ubiquitous metabolites have been identified in salmon muscle: EQ quinone imine,[1] deethylated EQ[2] and EQ dimer (EQDM)[3] (Bohne et al., 2008), of which EQDM, the main metabolite, usually accounts for > 90% of the sum of EQ and EQDM (Lundebye et al., 2010; Bohne et al., 2008).

EQDM is regarded as an antioxidant in its own right (de Koning, 2002), and because EQDM is more lipophilic than EQ (Błaszczyk et al., 2013), it can more readily accumulate in liver and adipose tissue. The only study in the literature addressing the toxicity of EQDM *in vivo*, found no adverse effects on liver and kidney function in rats at a dose of 12.5 mg/kg body weight/day (Ørnsrud et al., 2011). However, the EQDM-induced transcriptional responses of phase I and II biotransformation enzymes appeared to be comparable to those reported for EQ (Ørnsrud et al., 2011), suggesting that EQDM and EQ may induce similar biotransformation pathways. Furthermore, similarly to EQ, EQDM has been reported to exhibit cytotoxic and genotoxic effects on human lymphocytes (Augustyniak et al., 2012). Still, the possible health risk of EQDM from dietary sources for consumers has yet to be characterized.

The aim of the present study was to investigate and characterize possible adverse health effects following 90 days dietary exposure to EQDM in male BALB/c mice. Six graded doses of EQDM were administered to the mice through the diet, and effects on health status were assessed in liver, kidney, spleen, blood and plasma.

A systems toxicology approach was employed in order to investigate the mode of action and underlying molecular mechanisms of dietary EQDM, using a multi-level -omics workflow as a screening tool to characterize EQDM-induced changes in hepatic metabolomic and proteomic profiles. The generated data were put into biological context using systems biology bioinformatic tools, and the significance of the metabolic pathways identified as potential targets of dietary EQDM for adverse outcomes was further consolidated using physiological and biochemical analyses of relevant toxicological endpoints. Moreover, guidance values for the upper level of intake of EQDM were derived using the benchmark dose (BMD) and the No-Observed–Adverse-Effect-Level (NOAEL) approach.

Using this integrated approach, we aimed to gain mechanistic insight and a quantitative understanding of the potential toxicity of dietary EQDM, and to contribute relevant knowledge for future risk assessments of EQDM in the food chain.

2. Materials and methods

2.1. Ethical statement

The animal facility and experiments were approved by the National Animal Research Authority at the Norwegian Food Safety Authority (approval identification no. 8835). Animal handling and experimental procedures were carried out in accordance with national and international ethical standards.

2.2. Experimental diets

Eight different feeds were produced; a control, six feeds spiked with EQDM and, for reference, one feed spiked with EQ. The feed composition is given in Table 1. EQDM was administered as a crystalline powder (> 95% purity; Synthetica AS, Oslo, Norway) mixed in a dry powder feed based on the purified AIN-93-M diet for maintenance of adult rodents. EQ (Capsoquin S-5162, 99% purity; courtesy of Industrial Técnica Pecuaria, S.A., Spain) was dissolved in the dietary oil and then blended into the dry diet. Ash, gross energy-, crude protein-, and total fat content were measured as previously described by Tastesen et al. (2014). The diets contained equal amounts of fat and protein, and were isocaloric.

2.3. Animals and feeding experiment

Eighty male BALB/c mice, six weeks of age, were obtained from Charles River (Germany). Following 10 days of acclimation on control diet (AIN-93-M; EQDM 0), a 90 day subchronic dietary exposure study was performed (in accordance with OECD guideline 408), using six doses of EQDM (0.1, 1, 100, 1000, 3000 and 5000 mg/kg feed), one dose of EQ (1000 mg/kg feed) and an unspiked control. The mice were housed individually and kept at room temperature (20–22 °C), with a relative humidity of 45–65% and a 12 h light/dark cycle (lights on 7a.m.). Throughout the experiment, the mice were monitored daily. Water and feed, available *ad libitum*, were changed three times per week and feed intake was recorded.

2.4. Body weight development and body composition

Body weight was recorded once a week. Whole body composition was determined at the start of the study and after 12 weeks using a nuclear magnetic resonance spectrometer (minispec LF50 Body Composition Analyzer mq 7.5, Bruker Optik GmbH, Germany).

Animals exposed to a single dose of EQ comparable to the highest dose of EQDM (EQDM 6) refused their feed and, after ten days, the mice had lost 11% of their initial body mass. The animals appeared otherwise healthy and showed an immediate reaction to the EQ-containing feed. Possibly, sensory properties (taste and odour) of EQ (Błaszczyk et al., 2013) caused the observed reduction in feed intake affecting the palatability at the given concentration. The dose of EQ was therefore reduced to 1000 mg/kg feed (Table 1). The animals accepted the lower dose and started gaining weight. Thereafter, body weight gain of animals in the EQ group was comparable to body weight gain in all of the other groups. However, due to the initial lag in growth, the body weight of animals in the EQ group remained markedly lower compared to EQDM-exposed mice until the termination of the experiment. Since differences between animals exposed to EQ and animals exposed to EQDM for any measured parameter could not be differentiated from effects resulting from the deviations in feed intake and the subsequent lower body weight, the animals exposed to EQ were excluded from the study. All data collected for EQ-exposed mice can be found in Supplementary file B.

2.5. Plasma and tissue sampling

Mice were sacrificed inducing pneumothorax under isoflurane anesthesia (Isoba vet, Schering-Plough, Denmark). Blood from cardiac puncture was collected in EDTA-coated tubes, and a complete blood cell count was performed on fresh whole blood using a VetScan HM5 hematology analyzer (Abaxis Europe GmbH, Germany). Plasma and red blood cells were separated by centrifugation (15 min at 2500 g and 4 °C Microlite Microfuge, Thermo Electron Corporation) and stored at −80 °C for further analyses. Organs were immediately dissected out, weighed and either snap-frozen in liquid nitrogen and stored at −80 °C, or fixed in 4% paraformaldehyde. No gross pathologies were observed in any of the animals.

2.6. Ethoxyquin (EQ) and ethoxyquin dimer (EQDM) measurements

EQ and EQDM were extracted from pooled samples of liver, spleen and kidney (n = 10/pool) with hexane after saponification in ethanol-NaOH, while EQ and EQDM from feed samples were extracted directly with 0.1% (w/v) solid acetic acid in acetonitrile. The concentrations of EQ and EQDM were quantified by reversed-phase high-performance liquid chromatography with fluorescence detection, using an external

[1] 2,6-dihydro-2,2,4-trimethyl-6-quinolone.
[2] 6-hydroxy-2,2,4-trimethyl-1,2-dihydroquinoline.
[3] 1,8′-bi(6-ethoxy-2,2,4-trimethyl-1,2-dihydroquinoline).

Table 1
Composition of the experimental diets fed to male BALB/c mice for 90 days.

Component	Dietary treatment							
	Control	EQDM 1	EQDM 2	EQDM 3	EQDM 4	EQDM 5	EQDM 6	EQ†
Stated								
Ethoxyquin dimer (mg/kg)[a]	0	0.1	1	100	1000	3000	5000	0
Ethoxyquin (mg/kg)[b]	0	0	0	0	0	0	0	(5000) 1000
Casein powder (g/kg)	140	140	140	140	140	140	140	140
Soy bean oil (g/kg)	40	40	40	40	40	40	40	40
Sucrose (g/kg)	100	100	100	100	100	100	100	100
Potatoe starch. dextrinized (g/kg)	125	125	125	125	125	125	125	125
Corn starch (g/kg)	496	496	496	496	496	496	496	496
L-Cystine (g/kg)	1.8	1.8	1.8	1.8	1.8	1.8	1.8	1.8
Cellulose (g/kg)	50	50	50	50	50	50	50	50
t-Butylhydroquinone (g/kg)	0.01	0.01	0.01	0.01	0.01	0.01	0.01	0.01
Mineral mix (g/kg)[c]	35	35	35	35	35	35	35	35
Vitamin mix (g/kg)[d]	10	10	10	10	10	10	10	10
Choline Bitartrate (g/kg)	2.5	2.5	2.5	2.5	2.5	2.5	2.5	2.5
Analyzed[e]								
Ethoxyquin (mg/kg)	< LOQ	< LOQ	0.02	3	27	69	115	(3743) 1049
Ethoxyquin dimer (mg/kg)	< LOQ	0.13	0.75	88	931	2501	4481	(< LOQ) 3
EQ & EQDM (mg/kg)	< LOQ	0.13	0.77	91	958	2570	4596	(3743) 1052
%EQ		0	2.7	3.4	2.9	2.8	2.6	(100) 99.7
Crude protein (N*6.25)	131	128	131	131	130	134	132	130
Lipid (g/kg)	39	41	41	41	41	40	38	41
Ash	30	30	30	33	30	30	28	30
Gross energy (kcal/g)	4.1	4.1	4.2	4.1	4.1	4.1	4.1	4.1

†Intended and measured concentration in feed before (given in parentheses) and after intervention.
[a] Synthetica AS, Oslo, Norway (> 95% purity).
[b] Capsoquin S-5162, Industrial Técnica Pecuaria, S.A., Spain (99% purity).
[c] AIN 93G MIN MIX (M) (product number 829912; Special Diet Services, Witham Essex, England).
[d] AIN-93-VX NCR95 compliant vitamin mix (product number 829905; Special Diet Services, Witham Essex, England).
[e] Analyzed values represent the mean of technical duplicates.

standard curve, as previously described by Bohne et al. (2007a), with modifications described by Ørnsrud et al. (2011).

Of note, the measurement of EQ and EQDM revealed presence of ca. 3% EQ of the sum of EQ and EQDM in each of the EQDM-spiked experimental diets (Table 1), which were confirmed as residues from the synthesized EQDM powder. According to previous reports, EQ typically accounts for a minor part of the sum EQ and EQDM found in farmed Atlantic salmon fillets exposed to EQ through their diet and reared according to commercial farming practice (Bohne et al., 2008; Lundebye et al., 2010). Although not optimal in terms of experimental design, the presence of minor concentrations of EQ may be considered as relevant for human exposure.

2.7. Liver metabolomic profiling

In order to identify possible effects on liver metabolism, global metabolite profiles were determined in individual liver samples of three randomly chosen mice from each experimental exposure group. Semi-quantitative metabolomic analysis was performed by Metabolon Inc. (NC, USA), according to Metabolon's standard methods. Briefly, after addition of recovery standards, samples were extracted and prepared for analysis using the automated MicroLab STAR® system (Hamilton Company, NV, USA). The extracted samples were subsequently divided into four fractions and analyzed using a combination of reverse-phase ultra-performance liquid chromatography mass spectrometry (UPLC-MS/MS) with positive and negative ion mode electrospray ionization (ESI), and hydrophilic interaction (HILIC) UPLC-MS/MS with negative ion mode ESI along with several internal standards. All methods utilized a Waters ACQUITY UPLC and a Thermo Scientific Q-Exactive high resolution/accurate mass spectrometer coupled to a heated ESI source and an Orbitrap mass analyzer operated at 35 000 mass resolution. The MS analysis alternated between MS and data-dependent MS^n scans using dynamic exclusion and the scan range covered 70–1000 m/z.

Instrument variability was 4% for liver tissue internal standards, and total process variability for endogenous metabolites was 8% in the samples. Known compounds were identified by comparison to metabolomic library entries of purified standards.

2.8. Liver proteomic profiling

To further investigate possible effects on molecular pathways, proteomic profiles were determined in liver samples. To facilitate integration of the protein and metabolite profiles, individual samples from the same three mice previously chosen for metabolomics analyses were used for the proteomic profiling. Sample preparation, protein identification and quantification were performed at the Proteomics Unit at the University of Bergen, Norway (PROBE), according to standardized protocols. In brief, 20–50 mg liver samples were incubated at 95 °C for 7 min in 10 µl lysis buffer/mg tissue (4% SDS, 0.1M Tris-HCl, pH 7.6) and then lyzed by sonication, using a ultrasonication rod (Q55 Sonicator, Qsonica, CT, USA) at 30% amplitude for 30 s, or until tissue was dissolved. The lysed tissue was centrifuged for 10 min at 13000 rpm and the supernatant was collected for determination of protein concentration using a Pierce™ BCA Protein assay kit (Thermo Scientific). 1M DiThiotreitol was added to the lysates, to obtain a final concentration of 0.1M, and the mixture was incubated at 95 °C for 5 min. The samples were further processed using a Filter Aided Sample Preparation (FASP) protocol with trypsin digestion as described by Wiśniewski et al. (2009).

Between 0.5 and 1 µg protein (as tryptic peptides dissolved in 2% acetonitrile and 0.1% formic acid) was injected into an Ultimate 3000 RSLC system (Thermo Scientific, CA, USA) connected online to a linear

quadrupole ion trap-orbitrap (LTQ-Orbitrap Elite) mass spectrometer (Thermo Scientific, Bremen, Germany) equipped with a nanospray Flex ion source (Thermo Scientific). Samples were loaded and desalted on a pre-column (Acclaim PepMap 100, 2 cm × 75 μm ID nanoViper column, packed with 3 μm C18 beads) at a flow rate of 5 μl/min for 5 min with 0.1% trifluoroacetic acid. Peptides were separated using a biphasic acetonitrile gradient from two nanoflow UPLC pumps (flow rate of 270 nl/min) on a 50 cm analytical column (Acclaim PepMap 100, 50 cm × 75 μm ID nanoViper column, packed with 3 μm C18 beads). Solvent A and B were 0.1% trifluoroacetic acid (vol/vol) in water and 100% acetonitrile, respectively. The gradient composition was 5%B during trapping (5 min) followed by 5–7% B (over 1 min), 7–21% B (134 min), 21–34% B (45 min), and 34–80% B (10 min). Elution of very hydrophobic peptides and conditioning of the column were performed during 20 min isocratic elution with 80% B and 20 min isocratic elution with 5% B respectively.

The eluting peptides from the LC-column were ionized in the electrospray and analyzed by the LTQ-Orbitrap Elite. The mass spectrometer was operated in the data-dependent-acquisition (DDA)-mode to automatically switch between full scan MS and MS/MS acquisition. Instrument control was through Tune 2.7.0 and Xcalibur 2.2. Survey full scan MS spectra (from m/z 300 to 2.000) were acquired in the Orbitrap with resolution R = 240 000 at m/z 400 (after accumulation to a target value of 1e6 in the linear ion trap with maximum allowed ion accumulation time of 300 ms). The 12 most intense eluting peptides above an ion threshold value of 3000 counts, and charge states 2 or higher, were sequentially isolated to a target value of 1e4 and fragmented in the high-pressure linear ion trap by low-energy collision-induced-dissociation (CID) with normalized collision energy of 35% and wideband-activation enabled. The maximum allowed accumulation time for CID was 150 ms, the isolation with maintained at 2 Da, activation q = 0.25, and activation time of 10 ms. The resulting fragment ions were scanned out in the low-pressure ion trap at normal scan rate, and recorded with the secondary electron multipliers. One MS/MS spectrum of a precursor mass was allowed before dynamic exclusion for 40s. Lock-mass internal calibration was not enabled.

Prior to statistical analysis, the proteomics data were further processed using MaxQuant as described by Tyanova et al. (2016). In short, MaxQuant (Cox and Mann, 2008) running the built-in search engine Andromeda (Cox et al., 2011) and protein sequences of the complete mouse proteome downloaded from Uniprot (Magrane and UniProt Consortium, 2011) were used for protein identification and quantification. For protein identification, carbamidomethylation of cysteines and protein N-terminal acetylation as well as oxidation of methionines were set as fixed modification and variable modification, respectively. Precursor mass tolerance was set to 4.5 ppm and 20 ppm were used for fragment ion identification. Up to two missed cleavages were allowed for trypsin digestion. Within MaxQuant, the software option “Match between runs” was enabled. The false discovery rates (FDR) for peptide and protein identification were set to 1%. Only unique peptides were used for label-free quantification (LFQ) according to the method described by Cox et al. (2014). Relevant protein expression data including LFQ intensities, statistical significance, fold changes, and protein identification features including accession numbers, protein names, isoelectric point, molecular weight, as well protein identification metrics are provided in Supplementary file A, Tables S16 and S17.

2.9. Histopathological evaluation of liver, spleen and kidney tissue

Following dissection, liver, spleen and kidney tissue were fixed in neutral buffered formaldehyde (4%) and shipped to the Pathology section at the Norwegian Veterinary Institute for histopathological evaluation. The fixed tissue samples were dehydrated, paraffin embedded, sectioned (3 μm) and stained with hematoxylin and eosin (H&E) for morphological evaluation. The histopathological findings were categorized according to severity or characteristics and number of animals in each category was recorded. Histopathological evaluation was performed blinded by two pathologists. The results are presented as quantal data (% presence).

2.10. Plasma biochemistry

Plasma concentrations of biochemical markers, including albumin, total protein, glucose, total cholesterol, alanine aminotransferase (ALT), aspartate aminotransferase (AST), alkaline phosphatase, bile acids, bilirubin, creatinine, urea, triacylglycerides (TAG) and free fatty acids (FFAs) were measured with an automated MaxMat PL II diagnostic analyser system (MAXMAT S.A., Montpellier, France) using kits from DIALAB GmbH (Neudorf, Austria) and MaxMat (Montpellier, France).

Concentrations of plasma sodium and chloride were determined using an ABL 77 blood gas and electrolyte analyzer (Radiometer Copenhagen, Denmark).

2.11. Redox status in liver

In order to assess changes in redox status and presence of oxidative stress in the liver, the concentrations of reduced and oxidized glutathione (GSH and GSSG, respectively), Vitamin E and thiobarbituric acid reactive substances (TBARS) were quantified in liver tissue. For quantification of GSH and GSSG, frozen liver tissue samples were weighed and homogenized in either 4x volume (v/w) of ice-cold 0.9% saline buffer (9 g/L NaCl in ddH_2O), or 2x volume (v/w) of ice-cold thiol scavenger (*N*-ethylmaleimide pyridine derivative solution, Cat. No. GT35c; Oxford Biomedical Research, MI, USA) diluted 3:7 in 0.9% saline buffer, respectively, using a ball mill (25 rpm for 1–2 min; Retsch MM301 ball mill, Haan, Germany). The homogenates were centrifuged (5 min, 1500*g*, 4 °C), and GSH and GSSG were measured in the supernatant using the Cuvette Assay kit for GSH/GSSG (Cat. No. GT35; Oxford Biomedical Research, MI, USA) following the manufacturer's instructions.

Vitamin E was extracted from homogenized pools of liver samples (n = 10/pool) from all animals in each exposure group with hexane, after saponification with ethanol/KOH. Alpha-tocopherol concentrations were quantified by high-pressure liquid chromatography with fluorescence detection, using an external standard curve as described by Lie et al. (1994).

Finally, lipid peroxidation was assessed through measurement of TBARS in individual liver samples of four randomly chosen mice from each experimental exposure group. The concentrations of TBARS were determined spectrophotometrically as described by Hamre et al. (2001).

2.12. Liver lipid classes

Tissue lipids were extracted with chloroform:methanol, 2:1 (v/v) from individual liver samples of four randomly chosen mice from each exposure group, and lipid classes were quantified using High Performance Thin Layer Chromatography (HPTLC) according to the method previously described by Torstensen et al. (2011).

2.13. Statistical analyses and bioinformatic analyses of multi-level omics data

All statistical data analyses were performed using R (version 3.4.0 (R Core Team, 2017)). Data were analyzed employing one-way ANOVA followed by Tukey's test for multiple comparison of group means. Normal distribution of the model residuals and homogeneity of variance amongst treatment groups were tested with Shapiro-Wilk's test and Levene's *F*-test, respectively. Data not meeting the assumptions of ANOVA, were analyzed using Kruskal-Wallis’ test, and Wilcoxon's test for multiple pairwise comparison of group ranks. For measurement of

Table 2
Physical parameters of male BALB/c mice after 90 days dietary exposure to ethoxyquin dimer (EQDM). Results are presented as mean ± SD (n = 10, unless indicated otherwise; a: n = 7, b: n = 8, c: n = 9).

Parameter	*Dietary treatment*							ANOVA (*p*)
	Control	EQDM 1	EQDM 2	EQDM 3	EQDM 4	EQDM 5	EQDM 6	
Initial body weight (g)	21.0 ± 1.1	21.0 ± 1.1	21.0 ± 1.0	20.9 ± 1.0	21.0 ± 1.0	21.0 ± 1.0	21.0 ± 1.0	> 0.99
Feed intake (g)	299.4 ± 14.8	304.8 ± 10.3	296.6 ± 11.4	306.2 ± 9.0	291.5 ± 14.5	303.2 ± 12.4	296.2 ± 7.6	0.07
Total body weight gain (g)	8.7 ± 1.9	8.0 ± 1.9	8.9 ± 1.9	7.9 ± 1.5	8.8 ± 1.3	8.1 ± 1.8	7.0 ± 1.3	0.16
Final body weight (g)	29.7 ± 2.3	29.0 ± 1.8	29.9 ± 1.7	28.8 ± 1.7	29.8 ± 1.6	29.1 ± 1.7	28.0 ± 0.6	0.17
Estimated exposure EQDM (mg/kg BW/day)	< LOQ	0.015 ± 0.001	0.081 ± 0.005	10 ± 1	99 ± 5	286 ± 22	518 ± 15	
Estimated exposure EQ & EQDM (mg/kg BW/day)	< LOQ	0.015 ± 0.001	0.084 ± 0.005	11 ± 1	102 ± 5	293 ± 22	531 ± 15	
Body composition								
Total body fat (g)	6.5 ± 2.8	5.8 ± 2.6	7.1 ± 1.7	6.2 ± 2.7 c	7.0 ± 2.0	5.3 ± 2.6	5.2 ± 0.9	0.35
Total body fat (% of BW)	22.3 ± 8.6	20.4 ± 8.3	24.7 ± 4.9	21.3 ± 8.3 c	23.9 ± 5.8	18.5 ± 8.1	19.3 ± 3.0	0.37
Total lean mass (g)	18.9 ± 0.9	18.8 ± 0.6	18.7 ± 0.5	18.9 ± 0.4 c	19.0 ± 0.5	19.4 ± 0.8	18.8 ± 0.4	0.15
Total lean mass (% of BW)	66.9 ± 6.0	68.2 ± 5.8	65.1 ± 3.4	67.5 ± 6.0 c	65.9 ± 3.9	69.6 ± 5.1	69.4 ± 1.7	0.29
Organ weights								
Heart (g)	0.15 ± 0.01	0.14 ± 0.01	0.14 ± 0.02	0.14 ± 0.01	0.15 ± 0.02	0.15 ± 0.02	0.15 ± 0.01	0.73
Cardiosomatic Index (*100)	0.50 ± 0.03	0.49 ± 0.04	0.47 ± 0.04	0.50 ± 0.05	0.50 ± 0.04	0.50 ± 0.05	0.52 ± 0.05	0.46
Spleen (g)	0.077 ± 0.005	0.077 ± 0.005	0.082 ± 0.009	0.078 ± 0.008	0.079 ± 0.006	0.086 ± 0.012 c	0.081 ± 0.004	0.26
Spleenosomatic Index (*100)	0.26 ± 0.01	0.27 ± 0.01	0.27 ± 0.04	0.27 ± 0.03	0.26 ± 0.02	0.29 ± 0.03* c	0.29 ± 0.01*	< 0.01
Liver (g)	1.14 ± 0.12	1.14 ± 0.10	1.17 ± 0.11	1.19 ± 0.12	1.39 ± 0.10*	1.63 ± 0.18*	1.60 ± 0.11*	< 0.001
Hepatosomatic Index (*100)	3.84 ± 0.22	3.93 ± 0.21	3.91 ± 0.30	4.11 ± 0.24	4.66 ± 0.25*	5.60 ± 0.37*	5.71 ± 0.38*	< 0.001
Kidneys (g)	0.40 ± 0.04	0.39 ± 0.01	0.39 ± 0.03	0.40 ± 0.02	0.39 ± 0.01	0.39 ± 0.03 c	0.40 ± 0.02 c	0.89
Renalsomatic Index (*100)	1.35 ± 0.16	1.36 ± 0.11	1.31 ± 0.07	1.38 ± 0.10	1.30 ± 0.08	1.35 ± 0.12 c	1.41 ± 0.09 c	0.29
Brain (g)	0.39 ± 0.04 a	0.41 ± 0.03 a	0.42 ± 0.02 a	0.42 ± 0.02 a	0.41 ± 0.03 b	0.41 ± 0.02 b	0.41 ± 0.01 b	0.56
White adipose tissue mass (g)	1.60 ± 0.30	1.54 ± 0.39	1.68 ± 0.29	1.44 ± 0.44	1.62 ± 0.31	1.29 ± 0.33*	1.16 ± 0.13*	< 0.01
White adipose tissue mass (% of BW)	5.37 ± 0.67	5.25 ± 1.10	5.60 ± 0.78	4.93 ± 1.27	5.40 ± 0.78	4.42 ± 0.97*	4.13 ± 0.41*	< 0.01

EQDM exposed groups were compared by one-way ANOVA with Tukey's post-hoc test, or where appropriate Kruskal-Wallis and Wilcox' pairwise comparison. *p < 0.05 compared to the Control.; Abbreviations: BW, Body weight.

alpha tocopherol levels in pooled liver samples, a dose-response was tested on the means of two technical replicates by a simple linear regression model using the statistical software GraphPad Prism version 7.03 (GraphPad Software Inc.). Histological data were analysed by Pearson's (level of confidence 95%) followed by pairwise comparisons of treated groups with the control group using two-tailed Fisher Exact Test using GraphPad. Results are presented as mean ± standard deviation (SD).

The Qlucore Omics Explorer version 3.1 (Qlucore AB, Lund, Sweden) was used for data processing and statistical comparison of metabolomic and proteomic profiles. Original scale raw area counts of all biochemicals and proteins were re-scaled mean centering the individual count values for each respective biochemical, before log2 transformation. The data were analyzed using one-way ANOVA followed by planned contrasts, comparing the liver metabolite and protein profiles of each exposure group to the livers of unexposed animals. For all statistical analyses, a p-value < 0.05 was used as significance cut-off. The data were further explored by principal component analysis (PCA) and hierarchical cluster analysis (HCA).

For the intergrated biological pathway analysis, Kyoto Encyclopedia of Genes and Genomes (KEGG) and UniProt accession numbers of significantly (p < 0.05, ANOVA) altered metabolites and proteins were imported into the Ingenuity Pathway Analysis software suite (IPA; Quiagen, CA, USA). Biological network analysis (IPA Core Analysis with default settings) was performed on successfully mapped features followed by targeted IPA upstream and comparison analyses as described in Rasinger et al. (2014).

2.14. Benchmark dose (BMD) analysis

BMD analysis was performed on all measured endpoints according to the EFSA benchmark dose technical guidance (EFSA, 2017). Results were obtained using the EFSA BMD online application (under development; https://shiny-efsa.openanalytics.eu/app/bmd). Fitting benchmark dose models was based on the R-package PROAST (available from http://www.rivm.nl/en/Documents_and_publications/Scientific/Models/PROAST), versions 64.16 (continuous data) and 61.3 (quantal data). Model performance was evaluated based on the Akaike information criterion (AIC). A default value of 2 units difference between AICs is considered as the critical value by the EFSA (2017). BMD models were accepted when the AIC of a fitted model was lower than the AIC of the null model −2, and and the model with lowest AIC (AICmin) was lower than the AIC of the full model +2 (AICmin < AICfull+2) (EFSA, 2017). For endpoints representing measurements on a continuous scale, two models (model 3 and 5) were considered from the exponential and hill model families, and the model with the lowest AIC was selected as the model for calculating the BMD confidence interval, the lower bound is reported by BMDL and the upper bound by BMDU. Averaging results from a default set of fitted models, based on the methodology in Wheeler and Bailer (2008), was available for BMD analysis of quantal data and, as recommended (EFSA, 2017), applied to findings from histopathological evaluation of tissues.

The default benchmark response (BMR) of 5% was used as the starting point for model fitting of continuous data ($BMDL_{05}$). However, as described in the EFSA technical guidance, the level of response was adjusted where a wide confidence interval (BMDU/BMDL) indicated low precision of the estimates or based on biological considerations (EFSA, 2017), and the BMDLs for BMRs of 10% or 20% changes above the modelled background were considered ($BMDL_{10}$ and $BMDL_{20}$, respectively).

For quantal data (histology) the default BMR was defined as a specified increase in incidence over background, and a BMR of 10% (extra risk; $BMDL_{10}$) was used as described by EFSA (2017). A 90% confidence interval around the BMD was estimated for each endpoint, and a final confidence interval was derived using the lowest BMDL and the highest BMDU. Taking biological relevance into account, potentially critical endpoints were determined, and an overall critical BMDL was derived from the obtained set of BMD confidence intervals from these endpoints as a Reference Point/Point-of-departure. The raw data used for the analysis are available in Supplementary file A, Tables S1–6.

For the output of the model fittings for all parameters, see Supplementary file C.

3. Results

3.1. Physical parameters, hematology and tissue accumulation

To evaluate the potential toxicity of the EQ dimer (representing the major metabolite of EQ found in salmon muscle), male BALB/c mice (n = 80) were exposed to EQDM at doses ranging from 0.015 ± 0.001 (EQDM 1) to 518 ± 15 (EQDM 6) mg/kg body weight/day for 90 days (Table 2). Dietary exposure to EQDM did not affect feed intake or body weight gain (Table 2).

Crude body composition was assessed in an NMR analyzer. There were no differences in total body fat mass or total lean body mass among any of the groups. However, white adipose tissue mass (sum of epididymal-, retroperitoneal- and inguinal white adipose tissue) was significantly decreased ($p < 0.001$) in mice fed the EQDM 5 and EQDM 6 diets (Table 2). At the same time, the liver mass and hepatosomatic indices increased gradually in mice exposed to EQDM at doses above EQDM 3 ($p < 0.001$).

Compared to unexposed controls, a significantly increased spleenosomatic index ($p < 0.01$) was observed in animals exposed to EQDM 5 and EQDM 6 ($p < 0.01$ and $p < 0.001$, respectively), as well as in EQ exposed animals. No differences were observed in heart, kidney and brain masses or relative organ weights. Tissue measurements of EQDM and EQ in liver, spleen and kidney verified a dose-dependent accumulation in all tissues (Supplementary file A, Table S7).

In order to assess general health status, a complete blood cell count was performed (Supplementary file A, Table S8). Exposure to EQDM 5 and EQDM 6 resulted in a decreased volume percentage of red blood cells (hematocrit) compared to control animals ($p < 0.05$; 8.9 and 13.37% decrease in EQDM 5 and EQDM 6, respectively). The lower hematocrit levels were accompanied by gradually decreased mean corpuscular volume, whereas no differences in hemoglobin concentrations were observed (Supplementary file A, Table S8). No significant differences were observed among the groups in any other hematological parameters, including total and differential white blood cell count (Supplementary file A, Table S8). Further, the values for all measured parameters were within the normal range for male BALB/c mice ("Charles River Technical Resources: BALB/c Mouse" 2017). The described changes were therefore not classified as pathological.

3.2. Liver metabolomic profiling and pathway analysis

To further investigate the possible effects of dietary EQDM exposure on the liver, an in-depth hepatic metabolic screening was performed. Hepatic metabolite profiles of mice exposed to increasing dietary doses of EQDM were examined using PCA and HCA, revealing clear changes in metabolite profiles in livers from mice exposed to doses above EQDM 3 (Fig. 1A&B). Although the overall percentage of explained variance on the first two components was moderate (21% and 12%, respectively), the PCA revealed a clear separation based on the dose of dietary EQDM (Fig. 1A). Liver samples from mice exposed to low doses including EQDM 1, 2 and 3 grouped together with samples from non-exposed mice, whereas samples from mice exposed to doses higher than EQDM 3 formed an overlapping population separating along both components 1 and 2.

Of the 664 identified biochemicals, 184 compounds were significantly altered by dietary EQDM treatment ($p < 0.05$, ANOVA, Supplementary file A; Table S10 for individual p-values). Classification of significantly altered compounds using the KEGG superpathway annotations revealed a clear predominance of metabolites (62%) belonging to the "lipid" superpathway, followed by "amino acid" and "cofactors and vitamins", representing 21% and 6%, respectively, of all significantly affected metabolites (Fig. 1C).

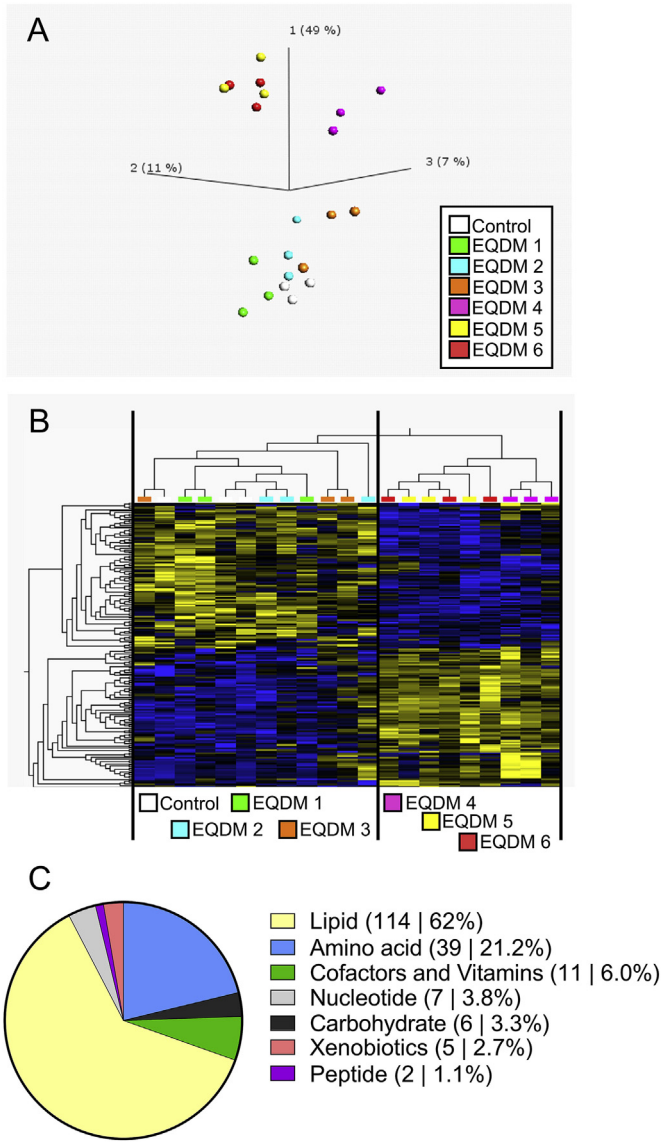

Fig. 1. Principal component analysis (PCA) and hierarchical clustering analysis (HCA) of significantly altered metabolites in livers of BALB/c mice exposed to increasing levels of ethoxyquin dimer (EQDM) through their feed. After 90 days of exposure, livers (n = 3) were sampled and subjected to metabolomics analysis. Differential analysis (ANOVA), PCA (A) and HCA (B) were performed using the Qlucore omics-explorer. For a complete overview of individual metabolites, see Supplementary file A, Table S9 (C) The relative abundance of significantly altered (ANOVA, $p < 0.05$) liver metabolites in different metabolite categories.

A dose-dependent increase in FFA levels was observed in livers from animals exposed to different doses of EQDM. EQDM 4 exposure led to increased levels of all measured FFAs, including palmitate (16:0), docosadienoate (22:2n-6) and docosatrienoate (22:3n-6; Fig. 2; Supplementary file A, Table S11). Increased levels of FFAs may result from increased fatty acid uptake, reduced fatty acid β-oxidation and/or hydrolysis of phospholipids or TAG. Significantly higher levels of a number of diacylglycerols and monoacylglycerols following a pattern similar to the FFAs (Fig. 2), indicated a contribution of TAG hydrolysis to the increased FFA pool.

The levels of some phospholipids, such as 14–16 GPCs, GPEs and 1-stearoyl-2-oleoyl-GPS (18:0/18:1), were reduced in mice exposed to doses higher than EQDM 3, whereas the levels of phospholipids including 20–22C fatty acids increased (Fig. 2; Supplementary file A, Table S11). However, a concomitant decrease of the phospholipid

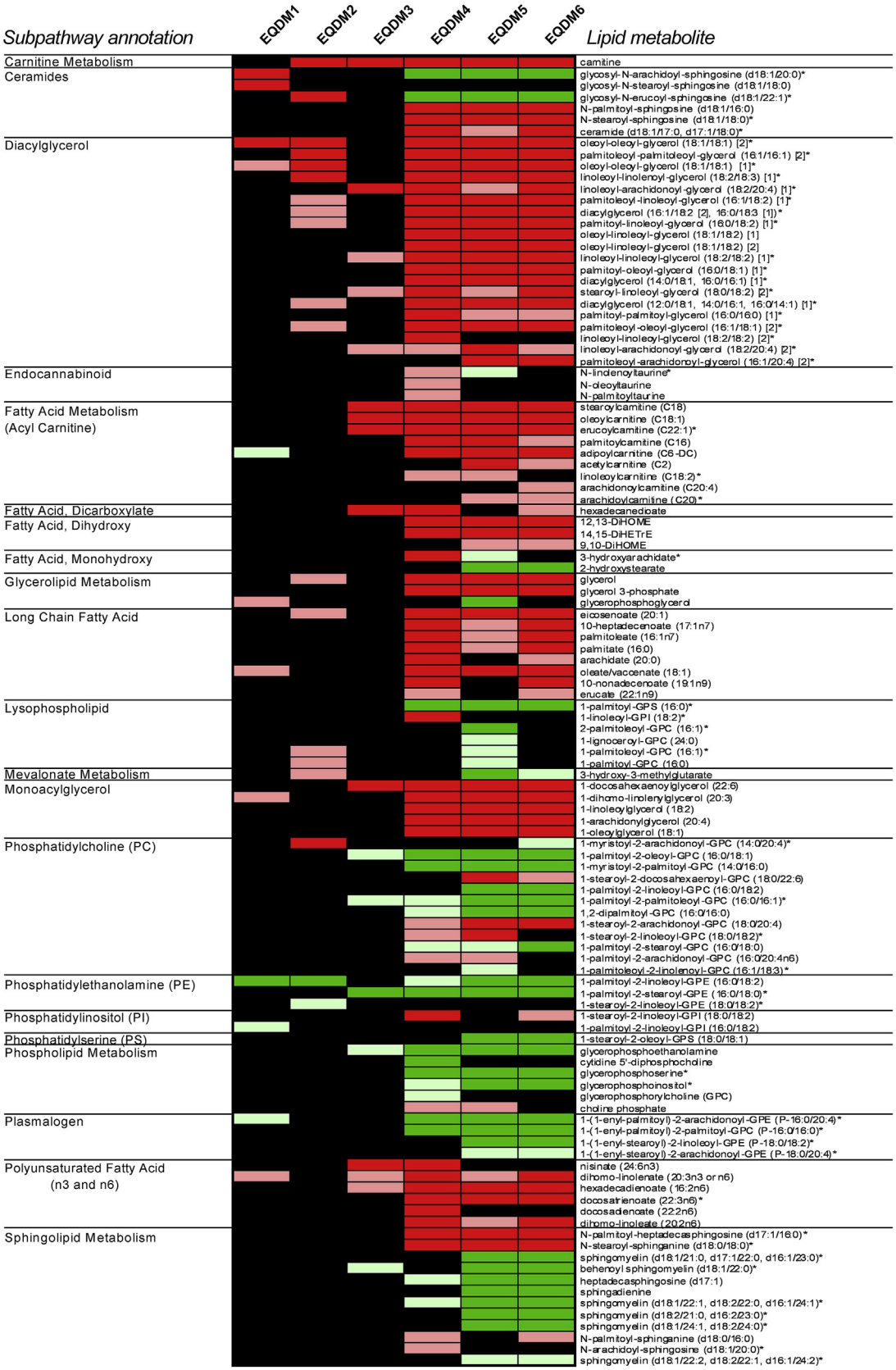

Fig. 2. Dose-dependent effects on hepatic lipid metabolism in male BALB/c mice exposed to increasing dietary levels of ethoxyquin dimer (EQDM) for 90 days. The heatmap shows the total of 114 individual lipid metabolites significantly increased (red) or decreased (green) at each exposure level, grouped according to their metabolic sub-pathway annotation. Scaled intensity means were used to calculate fold of increase or decrease of metabolites in each EQDM treatment group compared to unexposed control animals. Significance of difference was analyzed by *t*-test, with darker colours denoting significantly ($p < 0.05$) affected levels and light colours denoting a significance level of $p < 0.1$ compared to the control. Differences not meeting $p < 0.1$ are shown in black. For a complete list of calculated fold-changes and exact p-values, see Supplemental file A, Table S11. (For interpretation of the references to colour in this figure legend, the reader is referred to the Web version of this article.)

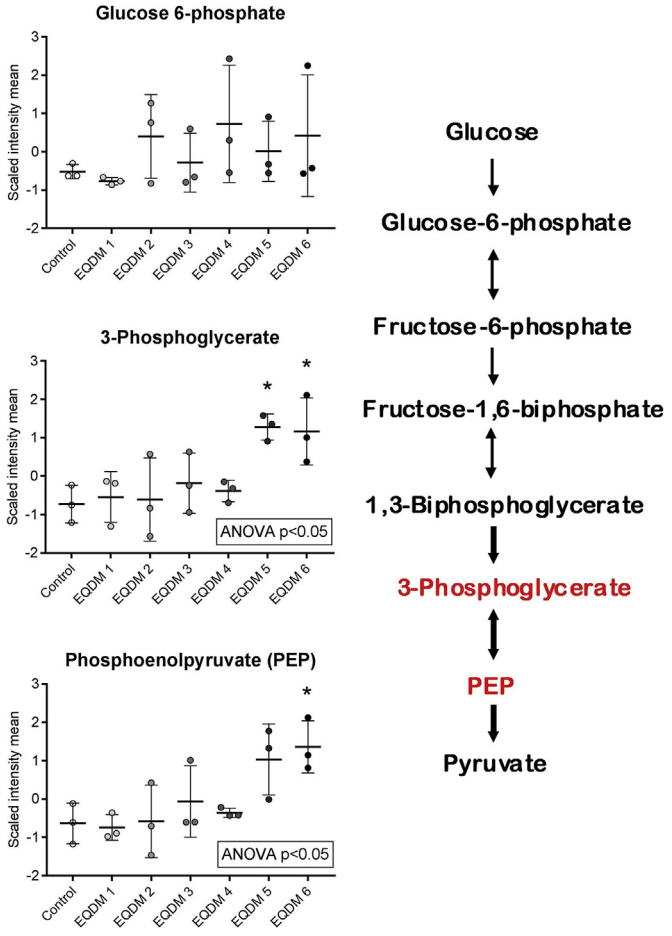

Fig. 3. Changes in levels of glycolytic metabolites in livers of mice exposed to increasing doses of ethoxyquin dimer (EQDM) during 90 days. The plots show scaled and mean centered intensities of the individual measurements in each experimental group (n = 3/group), in addition to the mean and standard deviation represented by a line and whiskers. Metabolites significantly affected by EQDM treatment (ANOVA) were further analyzed by *t*-test comparing each exposure group to the control. Statistical significance of pairwise comparisons is denoted with *p < 0.05 compared to the control.

breakdown products in mice exposed to doses higher than EQDM 3, suggested that phospholipid breakdown did not contribute to increased FFA levels.

Finally, high levels of FFAs may also result from decreased β-oxidation. Mitochondrial fatty acid oxidation requires conversion of acyl-CoA to acylcarnitine, and the levels of both long- and short chain acylcarnitines were increased in a dose-dependent manner in the livers of EQDM treated mice (Fig. 2). Concomitantly, the levels of the ketone body 3-hydroxybutyrate were unaffected by EQDM treatment, whereas the levels of the dicarboxylate fatty acid hexadecanedioate were significantly increased, suggesting incomplete mitochondrial β-oxidation and channeling of fatty acids towards omega-oxidation in liver microsomes at doses above EQDM 3.

Further, increased levels of glycerol and glycerol-3-phosphate, as well as increased levels of 3-phosphoglycerate and phosphoenolpyruvat (PEP) were observed in mice exposed to doses higher than EQDM 4 (Fig. 3), indicating increased rates of glycolysis and/or inhibition of further metabolic reaction of glycolytic intermediates downstream. Taken together, the alterations of liver metabolite profiles in animals exposed to EQDM indicated mobilisation of energy stores, and a disruption of fatty acid β-oxidation in liver mitochondria.

The glutathione system is responsible for maintaining redox homoeostasis and preventing free radical damage in cells. A trend towards increased levels of reduced glutathione levels (GSH) was detected in mice exposed to EQDM 4 and EQDM 6 (Fig. 4). Notably, although cysteine levels were not affected by EQDM treatment, the levels of cysteine sulfinic acid and hypotaurine, both dependent on cysteine, were depleted in livers of mice exposed to EQDM doses above EQDM 3 (Fig. 4). Concomitantly, levels of the substrate for GSH synthetase, gamma-glutamylcysteine, were significantly increased (Fig. 4), suggesting a redistribution of cellular cysteine stores towards increased glutathione synthesis. Thus, the observed treatment-related changes on the glutathione system indicated a compensatory induction of redox capacity, due to depleted glutathione pools in the liver indicating a disruption of liver redox-homeostasis and presence of oxidative stress.

The levels of n-6 fatty acid derived dihydroxy fatty acids 12,13-DiHOME, and 14, 15-DiHETrE were significantly elevated in mice exposed to doses higher than EQDM 3 (Fig. 2). In addition, a trend towards increased levels of 9,10 DiHOME was observed ($p < 0.1$) after exposure to EQDM 5 and EQDM 6 (Fig. 2), indicating alterations in inflammatory signaling and redox balance in response to high levels of EQDM. In line with this, exposure to doses higher than EQDM 3 increased the levels of some ceramides, including N-palmitoyl-sphingosine (d18:1/16:0), N-stearoyl-sphingosine (d18:1/18:0)* and ceramide (d18:1/17:0, d17:1/18:0)*, which can be produced by oxidative damage to sphingomyelins and as such are lipid markers of oxidative stress (Fig. 2). The levels of sphingomyelin decreased in livers of animals exposed to EQDM at levels higher than EQDM 4 (Fig. 2). Further, the levels of plasmalogens, a class of phospholipids that are susceptible to oxidative damage by free radicals, decreased concurrently. At the same time, EQDM exposure at doses higher than EQDM 3 lead to a depletion of Vitamin E (α-tocopherol and γ-CEHC glucuronide), which act as lipid antioxidants (Fig. 5). Together, these results indicate that exposure to high doses of EQDM leads to increased lipid peroxidation in the liver.

To verify these findings, liver oxidative status was assessed through direct measurement of concentrations of Vitamin E, TBARS, GSH and GSGG. Measurement of hepatic alpha-tocopherol concentrations confirmed a linear dose-dependent depletion following EQDM exposure ($y = -0.004$ mg/kg ww*Dose + 44.33, $F(1,5) = 7.559$, $p < 0.05$, R^2 of 0.602; Table 3). Direct measurement of hepatic GSH and GSSG confirmed a dose-dependent increase in GSH and GSSG levels ($p < 0.01$, ANOVA; Table 3), which reached significance in animals exposed to doses above EQDM 4 ($p < 0.05$, ANOVA). The presence of TBARS in the mice livers was generally very low, and levels were not affected by EQDM exposure.

3.3. Liver proteomic profiling and pathway analysis

In order to further investigate the mode of action of dietary EQDM, proteomic profiling was performed in liver samples. PCA revealed clear dose-dependent effects of dietary EQDM exposure on liver proteome profiles (Fig. 6A). Samples from animals exposed to doses lower than EQDM 3 formed a cluster with minor separation of samples from animals exposed to both EQDM 1 and EQDM 2 from control animals along the third component (5% of explained variance). Samples from animals exposed to EQDM 3 moderately separated along the first component (59% of explained variance), forming an individual cluster close to the samples of animals exposed to the lower doses, whereas samples from animals exposed to EQDM 4 showed a distinct separation along the first component.

Samples from animals exposed to doses above EQDM 4 separated further along the first component and formed an overlapping population. HCA echoed the distinct differences observed in the PCA between animals exposed to low doses (including EQDM 3) and animals exposed to higher doses (Fig. 6B). Also in agreement with the PCA, samples from animals exposed to EQDM 3 clustered together with samples from animals exposed to the lower doses, indicating that minor changes occured in the liver proteome following EQDM exposure at low dose

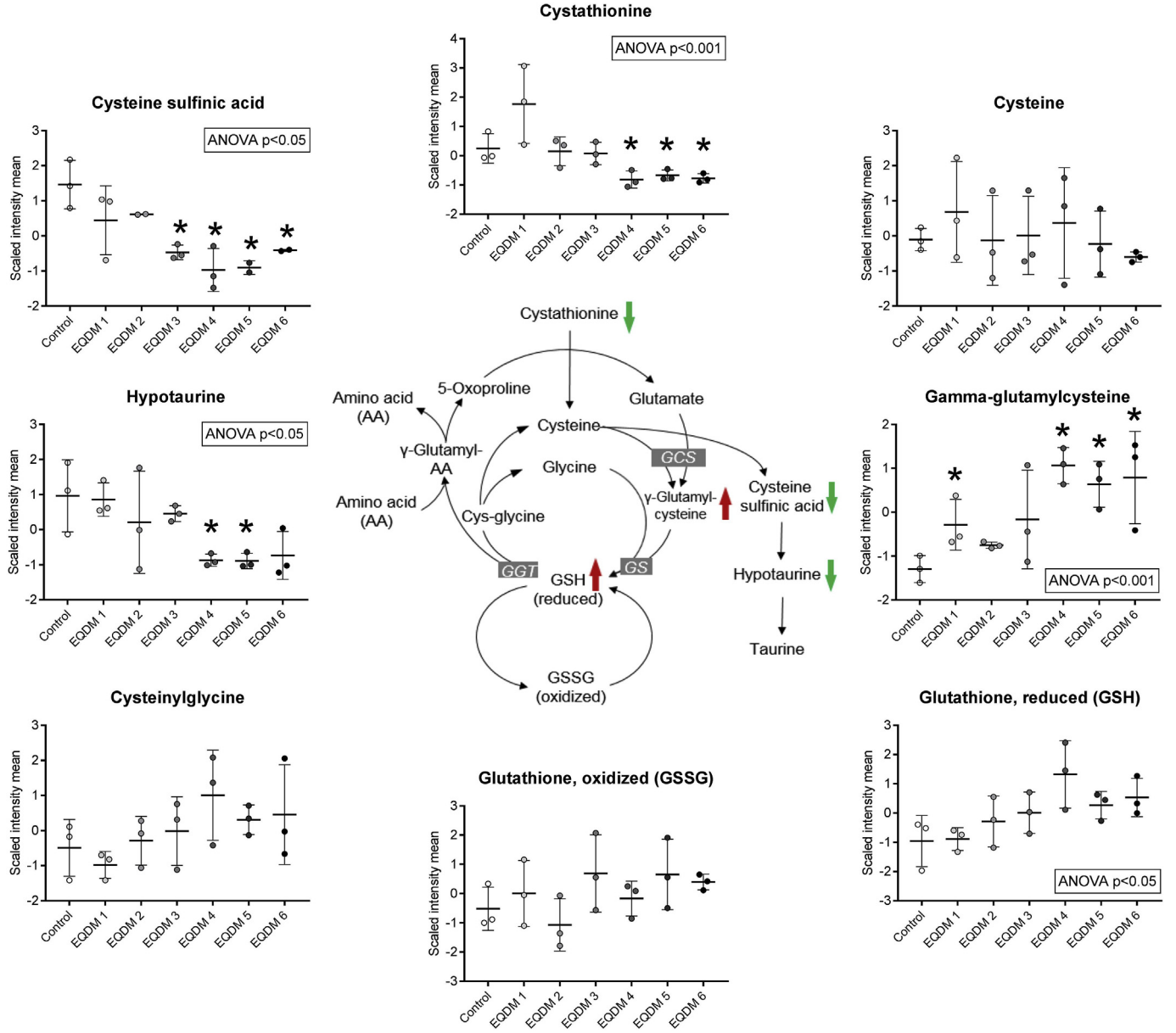

Fig. 4. Treatment-related alterations in metabolites connected to cysteine and glutathione metabolism in livers of mice exposed to increasing levels of ethoxyquin dimer (EQDM) through their diet for 90 days indicated changes in redox homeostasis and increased GSH biosynthesis. The plots show scaled and mean centered intensities of the individual measurements in each experimental group (n = 3/group), in addition to the mean and standard deviation represented by a line and whiskers. Metabolites significantly affected by EQDM treatment (ANOVA) were further analyzed by a *t*-test comparing each exposure group to the control. Statistical significance of pairwise comparisons is denoted with *p < 0.05 compared to control.

levels. Samples from animals exposed to EQDM 4 formed an individual cluster displaying substantial changes in proteome profiles similar to animals exposed to EQDM 5 and EQDM 6.

Of the 2246 detected and quantified proteins, expression levels of 504 identified proteins were significantly regulated by EQDM treatment ($p < 0.05$; Supplementary file A, Table S17). To obtain insight into the biological function of the alterations in the proteome profile observed after EQDM treatment at increasing doses, proteins detected at different abundances than in control animals (433; Supplementary file A, Table S17) were grouped into larger functional categories, using the Ingenuity Pathway Analysis (IPA) (Supplementary file A, Tables S19A–F). Similar to the differences observed in individual protein expression profiles induced by EQDM treatment at different doses, distinct dose-dependent responses were also detected at the pathway level, displaying a clear onset of systemic responses after exposure to doses above EQDM 3.

Enrichment analysis of altered proteins against canonical pathway annotations in IPA revealed a significant overlap of treatment-related changes in protein expression of several pathways (Fig. 7A). These included pathways related to mitochondrial function ("mitochondrial dysfunction", "oxidative phosphorylation"), amino acid degradation, energy metabolism ("TCA cycle II (eukaryotic)", xenobiotic metabolism ("xenobiotic metabolism signaling", "PXR/RXR activation"), "estrogen biosynthesis" and "fatty acid beta-oxidation I". Closer examination of altered proteins associated with the canonical pathway „mitochondrial dysfunction" in a network view suggested a disruption of the mitochondrial respiratory chain (Fig. 7B). Causal network analysis of protein expression data, where the directionality of the changes was taken into account, highlighted a dose-dependent induction of the "NRF2-mediated oxidative stress response" (z-score > 2) at doses above EQDM 3, whereas "PPARa/RXRa activation" was inhibited (z-score < 0) at doses above EQDM 4 (Fig. 7C).

To further elucidate the molecular mode of action of EQDM, an

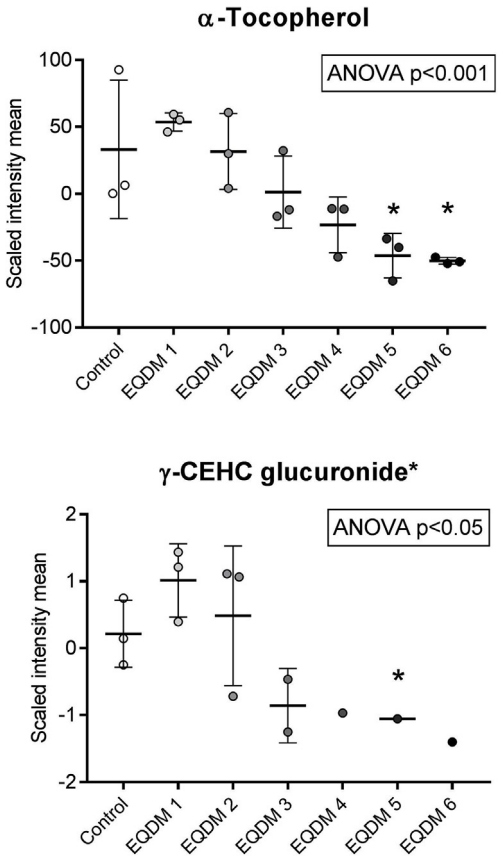

Fig. 5. Dose-dependent decrease of alpha-tocopherol and gamma-CEHC glucuronide, both important lipid anti-oxidants, in livers of mice exposed to increasing levels of ethoxyquin dimer (EQDM) through their diet for 90 days. The plots show scaled and mean centered intensities of the individual measurements in each experimental group (n = 3/group), in addition to the mean and standard deviation represented by a line and whiskers. Metabolites significantly affected by EQDM treatment (ANOVA) were further analyzed by a *t*-test comparing each exposure group to the control. Statistical significance of pairwise comparisons is denoted with *p < 0.05 compared to control.

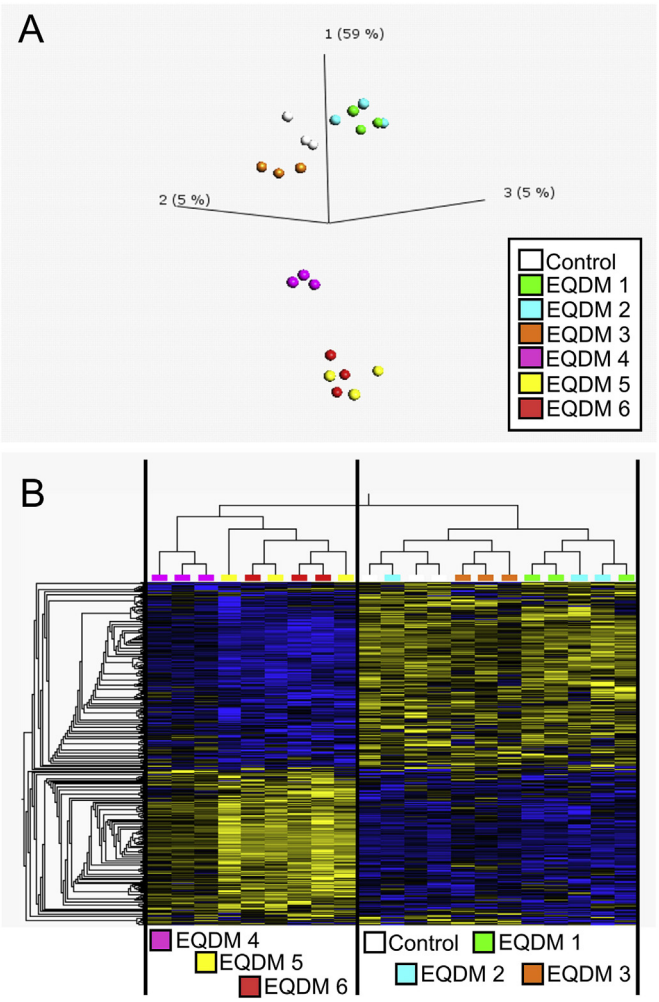

Fig. 6. Principal component analysis (PCA) and hierarchical clustering analysis (HCA) of significantly regulated (p < 0.05, ANOVA) proteins in livers of BALB/c mice. Mice were fed diets spiked with ethoxyquin dimer (EQDM) at increasing doses. After 90 days of exposure, livers (n = 3) were sampled and subjected to proteomics analysis. Differential analysis (ANOVA), PCA (A) and HCA (B) were performed using the Qlucore omics-explorer. See Supplementary file A, Table S16 for a complete overview of individual proteins.

upstream regulator analysis was performed in IPA. This indicated that changes observed in the liver following dietary EQ treatment were associated with dose-dependent activation of several transcription factors and ligand-binding nuclear receptors (Fig. 8A), highlighting a likely activation of NR1I2, NR1I3 and increasing PXR ligand-PXR-Retinoic

Table 3
Oxidative stress markers in livers of male BALB/c mice exposed to increasing levels of ethoxyquin dimer (EQDM) for 90 days. Results are presented as mean ± SD, n of individual measurements is given in parentheses. Liver α-tocopherol was measured in a sample pool of all animals for each exposure group (n = 1/group).

	Dietary treatment							P-values
	Control (n)	EQDM 1 (n)	EQDM 2 (n)	EQDM 3 (n)	EQDM 4 (n)	EQDM 5 (n)	EQDM 6 (n)	
Oxidative stress markers								
GSH (uM)	6613 ± 786 (10)	6386 ± 826 (10)	6786 ± 763 (10)	6970 ± 413 (10)	7256 ± 897 (10)	7310 ± 878* (10)	7667 ± 737* (10)	< .01
GSSG (uM)	11 ± 3 (10)	10 ± 2 (10)	12 ± 3 (10)	12 ± 2 (10)	14 ± 4* (10)	15 ± 3* (10)	15 ± 4* (10)	< .01
GSH/GSSG	667 ± 195 (10)	635 ± 136 (10)	572 ± 114 (10)	579 ± 122 (10)	543 ± 165 (10)	495 ± 99 (10)	175 ± 338 (10)	0.19
TBARS (nmol/g ww)	0.9 ± 0.3 (4)	0.9 ± 0.2 (3)	1.2 ± 0.2 (4)	1.0 ± 0.4 (4)	0.9 ± 0.4 (4)	1.0 ± 0.3 (4)	1.3 ± 0.5 (4)	0.67
Vitamin E (mg/kg ww)								
α-tocopherol	51.2	47.4	49.3	34.1	35.4	30.1	28.3	< .05†

EQDM exposed groups were compared by one-way ANOVA with Tukey's post-hoc test, or where appropriate Kruskal-Wallis and Wilcox' pairwise comparison. *p < 0.05 compared to the Control.
†The relationship between the dose of EQDM administered as predictor for hepatic α-tocopherol concentrations was tested in a simple linear regression model including all data points (n = 7): $Y = -0.003796*x + 44.33$, $R^2 = 0.6019$, $p < 0.05$.; Abbreviations: GSH; Glutathione (reduced), GSSG; Glutathione (oxidized), TBARS; Thiobarbituric acid reactive substances.

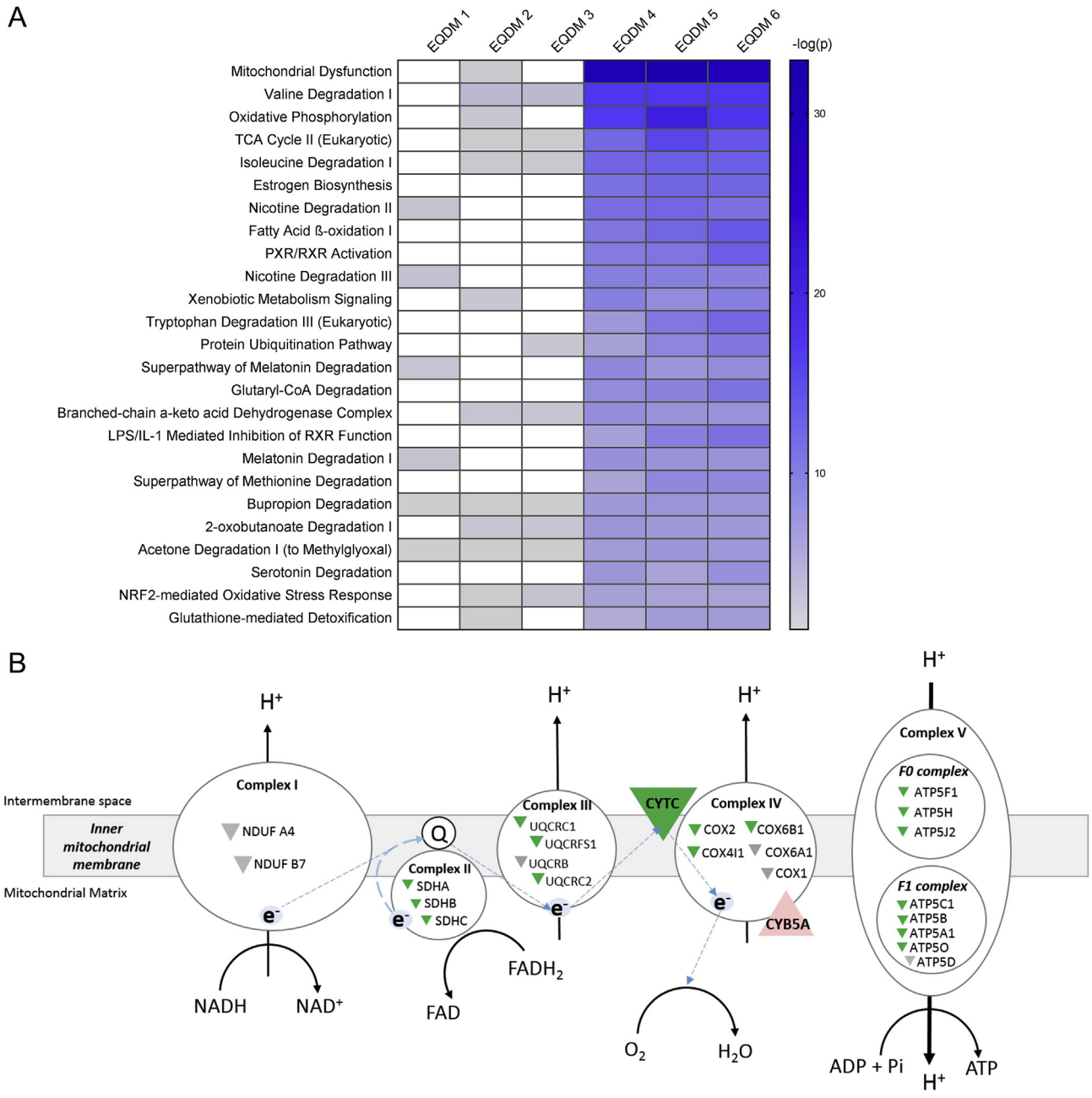

Fig. 7. Ingenuity pathway analysis on proteins altered by subchronic dietary exposure to increasing doses of ethoxyquin dimer (EQDM) in livers of male BALB/c mice. (A) According to the total number of affected proteins, the analysis revealed "Mitochondrial dysfunction", "oxidative phosphorylation", "fatty acid beta-oxidation I" among the top enriched canonical pathways. The top 25 pathways are presented. (B) Schematic overview over significantly elevated (▲) or lowered (▼ > EQDM 3; ▼ > EQDM 4) levels of proteins related to the canonical pathway "mitochondrial function", suggesting disruption of the mitochondrial respiratory chain in livers of mice exposed to higher doses of EQDM. (C) Furthermore, including the direction of changes highlighted a significant overlap for induction of the "NRF2-mediated oxidative stress response". For a full list of associated pathways, respective p-values of overlap and activation z-scores, see Supplementary file A, Table S19B.

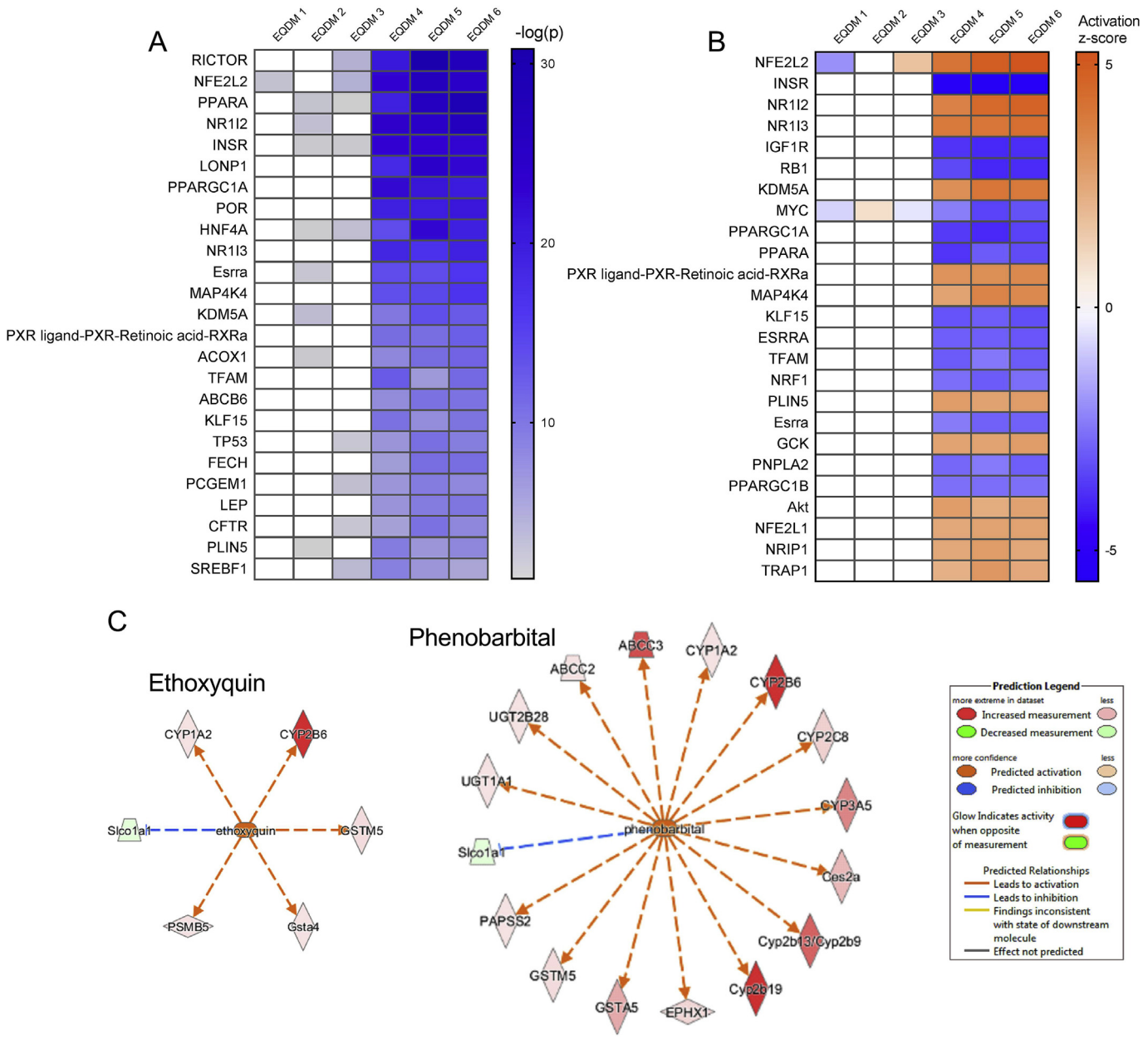

Fig. 8. Upstream regulator analysis (URA) of proteome changes induced by subchronic dietary exposure to increasing doses of ethoxyquin dimer (EQDM) in livers of male BALB/c mice. The transcriptional regulators from the regulator category "Genes, RNAs and proteins" were predicted from significantly altered levels of known targets from the IPA database (A). Taking direction of change into account, the analysis highlighted several likely upstream regulators from the category "genes, proteins and RNA", including the transcription factor NFE2L2 and the nuclear receptors NR1I2, NR1I3 and PPARA showing a significant overlap with responses described in the literature (B) The top 25 transcriptional regulators are presented. Results from the regulator category "drugs/chemicals" showed a significant overlap of regulated proteins with both a response induced by phenobarbital, as well as ethoxyquin (C). For an unfiltered output of the upstream regulator analyses, see Supplementary file A, Table S19E.

acid-RXR activity, as well as inhibition of PPARA at exposure levels above EQDM 3 (Fig. 8B). A dose-dependent effect was predicted for the transcription factor NFE2L2, with a significant overlap for decreased activity at the lowest exposure (EQDM 1) and a gradually increased activation after exposure to doses above EQDM 2 (Fig. 8B). Furthermore, the comparison of the EQDM-induced changes on protein levels with the literature compiled in the Ingenuity® Knowledge Base revealed a significant overlap with responses previously described for different drugs and chemicals, including phenobarbital and EQ (Fig. 8C).

3.4. Liver histopathology, lipid accumulation and oxidative stress status

Histological evaluation of liver sections revealed clear treatment related changes (Table 4) reflecting both observed alterations in the hepatic metabolite profile (Fig. 2) and changes in hepatic lipid measurements (Fig. 9A–B; Supplementary file A, Table S13), whereas no treatment-related effects were observed in a histopathological screening of spleen and kidney tissue (data not shown). In liver sections, microvesicular lipid accumulation, most often both centrilobular and midzonal, was observed in 50–60% of the animals exposed to EQDM at levels higher than EQDM 3 (Fig. 9C), whereas hepatic steatosis was observed in 0–10% of the animals belonging to the control group, exposed to the lowest dose of EQDM (EQDM 1) or EQ (Table 4). The lipid accumulation in each sample was not widespread, but rather observed as scattered areas. Single cell necrosis was observed in all groups (Fig. 9D). However, a significantly higher proportion of animals

Table 4
Histological evaluation of liver tissue after 90 days of dietary exposure to ethoxyquin dimer (EQDM).

Observation	*Dietary treatment*							*p-value*
	Control	EQDM 1	EQDM 2	EQDM 3	EQDM 4	EQDM 5	EQDM 6	
Steatosis	1/10	0/10	1/10	1/10	6/10	6/10	5/10	< 0.01
Steatosis microvesicular	0/10	0/10	1/10	1/10	2/10	3/10	5/10*	< 0.05
Steatosis macrovesicular	0/10	0/10	0/10	0/10	0/10	0/10	0/10	–
Steatosis mixed	1/10	0/10	0/10	0/10	4/10	3/10	0/10	< 0.05
Single cell necrosis	2/10	2/10	3/10	1/10	5/10	9/10*	7/10	< 0.01
Necrosis	2/10	3/10	2/10	2/10	5/10	8/10*	7/10	< 0.05
Mild	1/10	3/10	1/10	1/10	2/10	1/10	1/10	0.80
Moderate	1/10	0/10	1/10	1/10	3/10	1/10	3/10	0.39
Severe	0/10	0/10	0/10	0/10	2/10	6/10*	3/10	< 0.001
Accumulation of bile pigment	0/10	0/10	0/10	0/10	0/10	0/10	1/10	0.41

Frequencies of observations in EQDM exposed groups were compared using a Chi square test. A significant finding was further examined comparing each group to the control group using a two-tailed Fisher's Exact test. *$p < 0.05$ compared to the Control.

exposed to a higher dose than EQDM 3 had this lesion (Table 4).

Hepatic necrosis occurred as focal or multifocal lesions (Fig. 9D), and the degree of necrosis was assessed as follows: 0 = no necrosis observed, 1 = one necrotic focus (mild necrosis), 2 = two or three necrotic foci (moderate necrosis), and 3 = more than three necrotic foci (severe necrosis). Mild or moderate hepatic necrosis was observed in one to three animals in all groups, whereas severe necrosis was present in two to six animals exposed to doses of EQDM 4 and above (Table 4). Bile pigment (hepatocellular and canalicular) was not observed after EQDM exposure, except in one animal exposed to the highest dose (EQDM 6; 518 ± 15 mg EQDM/kg body weight/day).

As markers of impaired liver function and liver damage, ALT and AST levels were measured in plasma (Fig. 9E–F). Plasma ALT levels were significantly increased in animals exposed to EQDM at doses above EQDM 3 ($p < 0.05$), resulting in significantly lower ratios of AST/ALT ($p < 0.001$, Fig. 9G) in these groups. No changes were observed in other plasma markers of organ function (Supplementary file A, Table S14).

3.5. Benchmark dose assessment

The BMDL assessment was performed on average daily dose of EQDM (mg/kg body weight/day) versus quantitatively measured biological parameters (Table 5).

Clear treatment-related effects were observed for liver mass and hepatosomatic index, of which hepatosomatic index with a $BMDL_{05}$ 4.4 mg EQDM/kg body weight/day was the lower one. No trend was observed for spleen mass, but for the spleenosomatic index a $BMDL_{05}$ of 110 mg/kg body weight/day was established, which approximately corresponded to the NOEL for this parameter (99.4 mg EQDM/kg body weight/day). No BMD model could be fitted for kidney masses (Supplementary file C, Table S2).

The histopathological evaluation revealed morphological changes, including increased occurrence of microvesicular steatosis and increased presence of both single cell necrosis and necrotic foci in livers of mice exposed to doses higher than 10 mg EQDM/kg body weight/day (NOAEL), which indicated adverse physiological effects. At a dose level of 0.01 mg EQDM/kg body weight/day, increased occurrence of single cell necrosis had the lowest $BMDL_{10}$ of the histopathological parameters. Due to a very large BMDU/BMDL (< 10 000; Supplementary file C, Table S3), and thus very high uncertainty regarding the assessment, this finding was not considered for derivation of a critical BMDL. Occurrence of more than two necrotic foci („severe necrosis“) had the lowest BMDU/BMDL (18.3) ratio, and the $BMDL_{10}$ of 10.3 mg EQDM/kg body weight/day was thus the most reliable estimate. However, despite a higher BMDU/BMDL ratio, occurrence of microvesicular steatosis had the lowest $BMDL_{10}$ of 1.1 mg/kg body weight/day.

Accumulation of lipid in the liver was associated with mobilization of fatty acids from the adipose tissue stores. Thus, BMD confidence intervals were assessed for total liver lipid levels, the relative increase in liver TAG (Supplementary file C, Table S5) and decrease of white adipose tissue mass relative to body weight as adaptive responses and thus possible biomarkers of an adverse effect. Given that physiological parameters of energy homeostasis, including mobilization of fat from the adipose tissue stores to the liver for energy yield, show natural individual and temporal fluctuations, a 10% and 20% change from the modelled background response was considered as effect size for adipose tissue and liver lipid measurements (total amount of liver lipid and % liver TAG), respectively. The $BMDL_{10}$ for white adipose tissue mass relative to body weight was 11.7 mg EQDM/kg body weight/day. The lowest $BMDL_{20}$ was established at 4.5 mg EQDM/kg body weight/day for total liver lipid.

For plasma biomarkers of adverse effects, a model could only be fitted for the liver enzyme ALT and the ratio of AST/ALT (Supplementary file C, Table S4). Applying a default BMR of 5%, the plasma marker of adverse effect on liver, ALT had a rather high BMDU/BMDL ratio (9412.5), indicating an unreliable BMD assessment and was thus adjusted to 20%, providing a $BMDL_{20}$ of 1.9 mg EQDM/kg body weight/day. For the ratio of AST/ALT, a $BMDL_{05}$ was set at 5.7 mg EQDM/kg body weight/day.

Furthermore, BMDs were assessed for changes in liver GSH, vitamin E and TBARS levels. These parameters were not considered adverse effect markers, but rather markers of exposure and therefore not taken into account for evaluation of the critical BMDL. Given that physiological parameters of energy and redox homeostasis, show higher natural individual and temporal fluctuations, a 10% change from modelled background levels was applied. The BMD for increased GSH levels was the most reliable estimate with a BMDU/BMDL ratio ~23, and a $BMDL_{10}$ of 23.5 mg EQDM/kg body weight/day. For liver GSSG and liver vitamin E levels, applying a BMR at 10% resulted in a low confidence prediction of the BMD (Supplementary file C, Table S7). Applying a BMR of 20%, the confidence of the prediction for liver GSSG levels had a BMDU/BMDL of ~22 and a $BMDL_{20}$ of 10.0 mg EQDM/kg body weight/day. The lowest $BMDL_{20}$ for vitamin E levels was estimated to 0.2 mg EQDM/kg body weight/day. No model could be fit for liver TBARS (ALL AIC > AICnull).

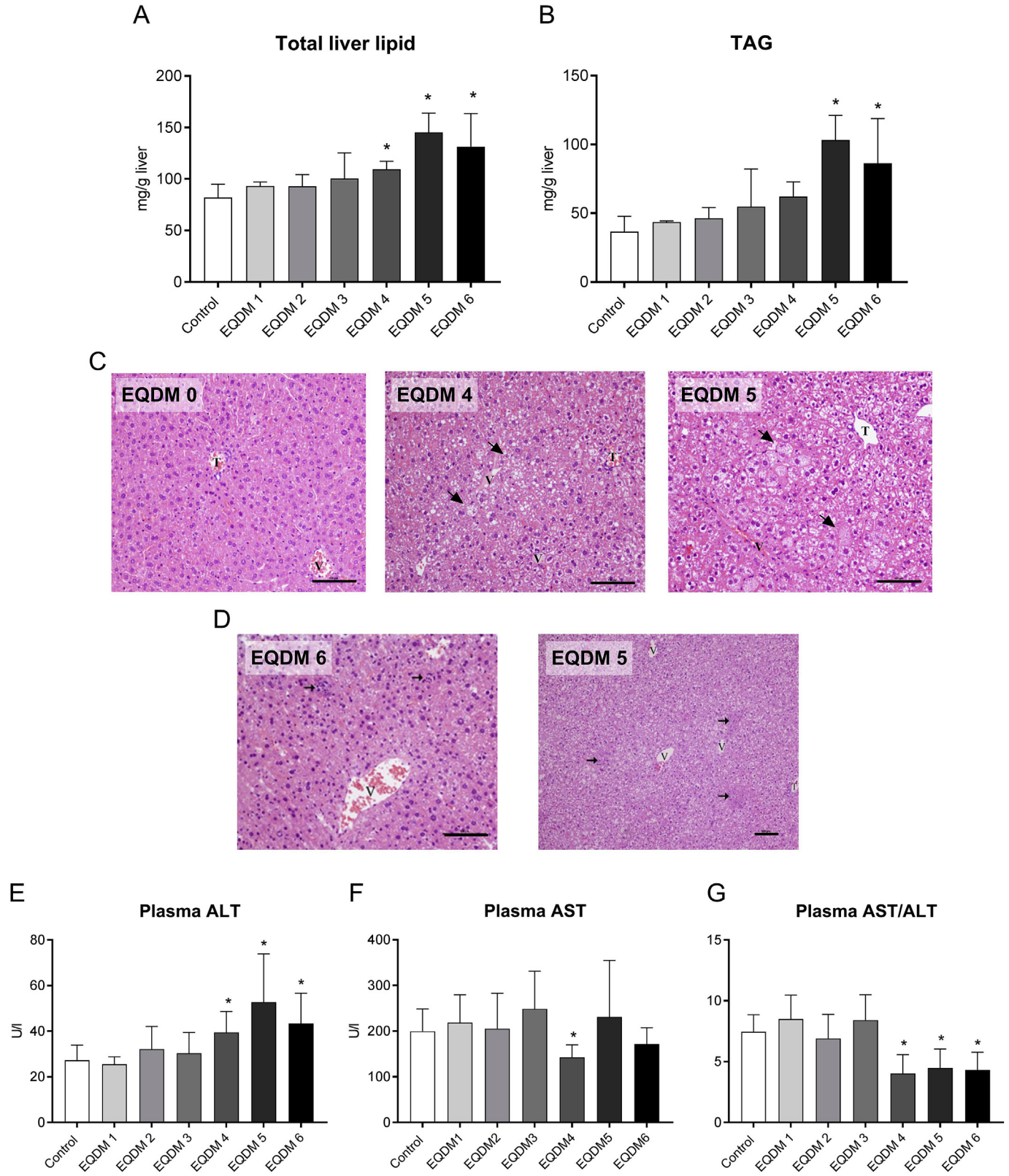

Fig. 9. Total lipids (A) and triacylglycerides (TAG; B) in livers of male BALB/c mice after 90 days of dietary exposure to increasing doses of ethoxyquin dimer (EQDM). (C) Liver tissue of mice fed control diet (EQDM 0- left panel), and mice exposed to doses above 10 mg/kg body weight/day displaying increased occurrence of centrilobular (mid panel) and midzonal (right panel) microvesicular steatosis (Table 4). H&E staining [scale bar: 100 μm]. (D) Liver tissue of mice exposed to doses above 10 mg/kg body weight/day had an increased frequency of single cell necroses (left panel) and presence of necrotic foci (right panel). H&E staining [scale bar: 100 μm]. Measurement of plasma alanine transferase (ALT; E), aspartate transferase (AST; F) and their ratio (G), indicated compromised liver function in mice exposed to higher doses of EQDM. Bar charts represent means ± SD of n = 4 (lipid measurements) and n = 8–10 (plasma markers of liver function). Statistical significant differences between EQDM exposed groups and control are indicated with *p < 0.05 (1-way ANOVA, Tukey's post hoc test).

Table 5
Benchmark doses (BMD) and lower and upper 90% confidence interval (BMDL and BMDU, respectively) for measured responses in male BALB/c mice exposed to seven doses of EQDM ranging from 0.015 to 518 mg/kg BW/day through their diet for 90 days. Taking biological variation into consideration, benchmark responses (BMR) were set at the default of 5%, or adjusted to 10 or 20%. For derivation of the critical BMDL, the width of the confidence interval was taken into account as an indicator of estimate precision. The No-observed-(adverse)-effect-levels (NOAEL/NOEL) were determined from statistical comparisons of responses in each predetermined dose group with the control group. From all endpoints assessed, the endpoints considered most biologically relevant (in bold) were included into assessment of the critical BMDL.

Endpoint	BMR (%)	BMD	BMDL lowest	BMDU highest	BMDU/BMDL	NOAEL/NOEL
Necropsy						
Liver weight	5	32.0	6.9	74.30	10.8	10
Liversomatic Index	**5**	**24.7**	**4.4**	**70.9**	**16.2**	**10**
Spleen weight	5	none	none	none		
Spleenosomatic Index	**5**	**200.0**	**110.0**	**334.0**	**3.0**	**99**
Kidney weight	5	none	none	none		
Renalsomatic Index	5	none	none	none		
Histopathology						
Microvesicular steatosis	**10**	**8.8**	**1.1**	**240.8**	**227.0**	**286**
Single cell necroses	**10**	**23.5**	**0.01**	**136.6**	**10155.9**	**99**
> 2 Necrotic foci observed	**10**	**42.6**	**10.3**	**188.0**	**18.3**	**99**
Liver lipid						
Total liver lipid	**20**	**12.1**	**4.5**	**125.0**	**28.0**	**10**
% Liver triacylglycerides	**20**	**143.0**	**49.8**	**599.0**	**12.0**	**10**
White adipose tissue mass	10	209.2	13.3	391.5	29.4	99
White adipose tissue mass/ body weight	**10**	**206.3**	**11.7**	**386.7**	**33.2**	**99**
Plasma biochemical markers						
Alanine transferase (ALT)	**20**	**48.2**	**1.9**	**108.0**	**58.1**	**10**
Aspartate transferase (AST)	20	none	none	none		
AST/ALT	**5**	**33.1**	**5.7**	**49.7**	**8.7**	**10**
Homeostatic responses redox homeostasis liver/Oxidative stress responses						
Reduced glutathione (GSH)	10	83.8	23.5	551.0	23.4	99
Oxidized glutathione (GSSG)	20	32.4	10.0	217.0	21.7	10
Liver alpha tocopherol	20	4.9	0.2	17.1	87.7	NA
TBARS liver	10	none	none	none		

Finally, for hematological parameters, showing high biological variability, a BMR of 10% was assessed. Although significant changes were observed for some hematological parameters comparing mice from the individual dose groups to the control mice, none of the measured parameters fulfilled the AIC criteria (Supplementary file C, Table S6), and the measurements were thus excluded from BMDL assessment.

An overview over the output, including the models, of the chosen parameters is given in Supplementary file C, Table S1. In conclusion, development of microvesicular steatosis was chosen as critical endpoint with the lowest $BMDL_{10}$ of 1.1 mg EQDM/kg body weight/day. Applying an uncertainty factor of 200 to the $BMDL_{10}$ we propose an ADI of 0.006 mg/kg body weight for dietary exposure to EQDM.

4. Discussion

EQDM is one of the main metabolites present in fish exposed to EQ through their feed, but health risks associated with dietary exposure to EQDM in consumers are largely uncharacterized. The present study investigated effects of subchronic dietary exposure to six doses of EQDM ranging from 0.015 to 518 mg/kg body weight/day in male BALB/c mice. Integrative analysis of classical physiological markers of toxicity and hepatic metabolite and proteome profiles revealed that dietary exposure to EQDM led to metabolic changes and disruption of whole body lipid metabolism at doses above 10 mg/kg body weight/day.

In line with previous results on dietary EQDM exposure in rats (Ørnsrud et al., 2011), in the present study, 90 days exposure to EQDM did not affect body weight in mice at doses up to 518 mg/kg body weight/day. However, a significant dose-dependent increase in relative liver mass was noted at doses of 99 mg EQDM/kg body weight/day and above (EQDM 4, EQDM 5, EQDM 6). Although overall body fat was not affected by EQDM treatment, a dose-dependent decrease in white adipose tissue mass was observed, which indicated a mobilization of lipids from adipose tissue stores and resulted in an accumulation of lipids in the liver.

The dose-dependent accumulation of liver TAG manifested as increased occurrence of microvesicular steatosis in animals given increasing doses of EQDM. Because of its central role in metabolism, the liver is an important target of toxicity for xenobiotics, and oxidative stress (Jaeschke et al., 2002; Gu and Manautou, 2012). Hepatic steatosis is a common consequence of toxic insult to the liver (Patel and Sanyal, 2013; Begriche et al., 2011). Hepatic microvesicular steatosis is a potentially severe liver lesion associated with drug-induced liver injury, which is caused by impairment of fatty acid metabolism (Begriche et al., 2011; Fromenty and Pessayre, 1995; Pessayre et al., 2010). In the present study, substantial changes in the hepatic metabolite profiles were observed following EQDM-exposure to doses of 99 mg/kg body weight/day and above (EQDM 4, EQDM 5, EQDM 6), including elevated levels of FFAs, reflecting increased lipid mobilisation through TAG hydrolysis and hepatic uptake of fatty acids in the liver. Of note, a dose-dependent accumulation of lipid intermediates, such as acylcarnitines in absence of increased levels of ketone bodies (Fig. 2), reflected a lipid profile typically associated with impaired mitochondrial fatty acid β-oxidation (Pessayre et al., 2012). Inhibited fatty acid β-oxidation may lead to increased levels of un-oxidized fatty acids in the liver. Non-

oxidized, non-esterified fatty acids are incorporated into TAG and accumulate in the form of small lipid droplets in the cytosol of hepatocytes, a hallmark of microvesicular steatosis (Begriche et al., 2006). Hence, EQDM-induced impairment of fatty acid β-oxidation, as suggested by proteomics and metabolomics analyses (Figs. 2 and 7) may have contributed to accumulation of liver TAG and the on-set of liver steatosis.

Increased frequency and severity of necrosis in livers of mice exposed to 99 mg/kg body weight/day and above, and concomitantly elevated ALT levels in plasma indicated progression of steatosis to steatohepatitis and thus an onset of liver damage. The mechanisms involved in the progression of steatosis to steatohepatitis in drug-induced liver damage are not well understood. However, it appears that mitochondrial dysfunction and cellular oxidative stress from overproduction of reactive oxygen species (ROS) play key roles in the pathogenesis of steatohepatitis (Begriche et al., 2011). The proteomics analyses revealed an EQDM-induced enrichment of features associated with mitochondrial dysfunction, mitochondrial oxidative phosphorylation and NRF2-mediated oxidative stress response. A number of steatohepatitis-inducing drugs are able to impair the mitochondrial oxidative phosphorylation process and inhibit the mitochondrial respiratory chain (Pessayre et al., 2012; Schumacher and Guo, 2015). Inhibition of fatty acid β-oxidation is reported to impair oxidative phosphorylation in the respiratory chain and ATP synthesis, and thereby increase production of ROS and oxidative stress (Begriche et al., 2011; Pessayre et al., 2012; Fromenty and Pessayre, 1995; Schumacher and Guo, 2015). Furthermore, high levels of FFAs and elevated levels of other lipid metabolites, including hydroxylated and dicarboxylic fatty acids as observed in livers of mice treated with EQDM, promote lipotoxic conditions, which can induce mitochondrial dysfunction (Fromenty and Pessayre, 1995, 1997; Begriche et al., 2011). Reduced energy availability and direct oxidative damage from ROS may, in more severe cases, induce hepatocyte necrosis (Begriche et al. 2006, 2011; Pessayre et al., 2012). EQ has been reported to interfere with energy-dependent mechanisms through inhibition of ATPase activity and disrupt electron transport in the mitochondrial respiratory chain in both liver and kidney of rats (Reyes et al., 1995; Hernández et al., 1993). Based on the pathway analysis performed in the present study (Fig. 7B), it appears, that also EQDM may disrupt the mitochondrial respiratory chain.

Depletion of vitamin E, particularly associated with the detoxification of reactive lipid species, in livers of EQDM-treated mice (Fig. 5 and Table 3), as well as elevated levels of lipid markers of oxidative stress (ceramides; Fig. 2) indicated increased rates of lipid peroxidation. Induction of oxidative stress is a hallmark of toxicity, and the generation of ROS is a natural consequence of xenobiotic biotransformation. EQDM is reported to be a biphasic inducer of xenobiotic metabolism (Ørnsrud et al., 2011), and may be biotransformed by liver microsomal enzymes (CYPs) through a series of redox reactions, which generates ROS (Guengerich, 2006; Klotz and Steinbrenner, 2017). In agreement with a previous study on the effects of EQ in mouse liver (Kim, 1991), EQDM exposure was found to increase levels of reduced liver glutathione (GSH; Fig. 4 and Table 3). A dose-dependent increase in oxidized glutathione levels (GSSG) in livers of mice exposed to EQDM at doses above EQDM 3, indicated perturbation of liver redox homeostasis. The observed concomitantly altered levels of cysteine-dependent metabolites and increased levels of γ-glutamylcysteine synthetase, the rate-limiting enzyme in glutathione biosynthesis (Fig. 4), suggested a compensatory induction of glutathione synthesis.

EQ-induced glutathione (GSH) synthesis and regeneration has been associated with the ability of EQ to activate the nuclear factor erythroid 2-related factor 2 (NRF2; also known as NFE2L2) signalling pathway (Hayes et al., 2000). Xenobiotics activate NRF2 through suppression of its negative regulator, KEAP1 (Kelch-like ECH-associated protein 1). KEAP1 may be oxidized by increased levels of cytosolic ROS or electrophiles originating from lipid peroxidation, which causes release of the NRF2 from the NRF2-KEAP1 complex and translocation to the nucleus. Subsequently, NRF2 activates transcription of target genes, including genes that encode phase II enzymes such as GSTs, UGTs, NADP(H):quinone oxidoreductase and epoxide hydrolase, as well as genes encoding proteins involved in antioxidant responses, including γ-glutamylcysteine synthetase, as observed in the present study (Kensler and Wakabayashi, 2010; Hayes et al., 2000; Shen and Kong, 2009). Using IPA as a bioinformatic tool, induction of the NRF2-mediated oxidative stress response was predicted to represent an important EQDM target pathway (Fig. 7C), indicating that EQDM may act in a similar manner to EQ.

Upstream regulator analysis based on hepatic proteomic profiles substantiated a significant overlap, predicting an activation of NFE2L2 by EQDM. This analysis further revealed that the changes observed in the liver proteome were likely associated with activation of the orphan nuclear receptors NR1I2 (also known as pregnane X receptor; PXR) and NR1I3 (also known as constitutive androstane receptor; CAR), as well as inhibition of peroxisome-proliferator activated receptor alpha (PPAR-α). The nuclear receptors PXR and CAR were originally characterized as xenosensors targeting enzymes of phase I and phase II metabolism of xenobiotics, but accumulating evidence demonstrates a distinct role of these receptors in maintaining energy homeostasis in the body (Wada et al., 2009; Gao and Xie, 2010). Activation of both PXR and CAR is associated with suppressed gene expression of PPAR-α (Wada et al., 2009), a master regulator of hepatic FA β-oxidation (Rao and Reddy, 2001), and PXR-mediated inhibition of PPAR-α has been linked to the development of microvesicular steatosis in transgenic mice (Zhou et al., 2006). Interestingly, dietary exposure to 0.5% w/w EQ was found to counteract the hepatocarcinogenic effect of ciprofibrate in rats (Rao et al., 1984). This could not be explained by an interference with peroxisome proliferation or peroxisome-associated enzymes (Lalwani et al., 1983). Yet, EQ-induced CYP enzyme induction in rat liver microsomes has previously been described as similar to the response produced by phenobarbital, a known CAR activator (Kahl and Netter, 1977). In fish, dietary exposure to EQ was found to induce expression of CYP3A mRNA (Bohne et al., 2007a). As expression of CYP3A mRNA in mammals is directly controlled by PXR (Staudinger et al., 2001; Xie et al., 2000), the authors speculated whether EQ or its metabolites may at least partly act through PXR mediated pathways (Bohne et al., 2007b). In agreement with our findings, no effect on regulation of *Cyp3a* expression or CYP3A activity was observed in rat livers following subchronic dietary exposure to a dose of 12.5 mg EQDM/kg body weight/day (Ørnsrud et al., 2011). However, in the present study, elevated protein levels of CYP3A5, CYP2B6 and CYP2C8, all direct targets of PXR, were observed at doses above 99 mg EQDM/kg body weight/day (Supplementary file A, Table S17). Thus, our data suggest that, in addition to activation of NRF2, EQDM potentially acts through induction of PXR/CAR-mediated pathways, including the PXR/CAR-induced inhibition of β-oxidation through suppression of PPAR-α expression and may ultimately cause steatohepatitis, if the exposure is continued.

4.1. Derivation of a health-based guidance value

Although an increase in relative spleen weights was noted, the most significant effect of dietary EQDM exposure appeared to be liver toxicity with a dose-dependent change in relative liver weight, which was associated with the development of microvesicular steatosis and necrosis. The hepatosomatic index had the lowest BMD and the most narrow 90% confidence interval ($BMDL_{05}$ of 4.4 mg EQDM/kg body weight/day), and was thus regarded the most reliable estimation. However, although the BMDs for histopathological findings were estimated with wider conficence intervals, as manifestations of treatment-related physiological changes, these endpoints were considered more critical in terms of biological relevance. In order to leave the largest possible margin of safety, the reference point was based on the lowest

BMDL for the most critical endpoint. Thus, occurrence of microvesicular steatosis with a $BMDL_{10}$ of 1.1 mg EQDM/kg body weight/day is proposed as a Reference Point for risk assessment.

The Reference Point from the toxicity study can be used to establish a health-based guidance value at which no adverse health effects are expected. Uncertainty factors are applied taking into account uncertainty and variability such as inter- and intraspecies differences, and commonly a default value of 200 is proposed for subchronic studies in rodents (EFSA, 2012). With the $BMDL_{10}$ of 1.1 mg EQDM/kg body weight/day as a reference point, and taking into account an uncertainty factor of 200, an ADI of 0.006 mg EQDM/kg body weight can be derived.

The proposed ADI of 0.006 mg EQDM/kg body weight, corresponds to an acceptable daily exposure of 0.36 mg EQDM/day for a 60 kg adult. For a person weighing 60 kg, eating one portion (300 g) of meat or fish, these food items may not contain more than 1.2 mg EQDM/kg (as the sole dietary source of EQDM). In the European Union, there are currently no Maximum Residue Limits (MRLs) established for EQ or its metabolites in food products of animal origin. Limited data is available on the occurrence of EQ and EQDM in various foods. Levels found in farmed Atlantic salmon fillet range between 0.33 and 1.45 mg EQDM/kg (Mean: 0.73 ± 0.29 mg/kg) (Lundebye et al., 2010; He and Ackman, 2000).

Of note, the measurement of EQ and EQDM in the feed used in the present study revealed presence of ca. 3% EQ of the sum of EQ and EQDM present in EQDM spiked feed. Although not optimal in terms of experimental design, the presence of minor concentrations of EQ may be considered relevant for human exposure, since EQ typically accounts for a minor part of the sum EQ and EQDM found in farmed Atlantic salmon fillets exposed to EQ through their diet and reared according to commercial farming practice (Bohne et al., 2008; Lundebye et al., 2010).

Based on the mean EQDM levels reported, consumption of 300 g farmed Atlantic salmon fillet would contribute approximately 61% to the proposed ADI. Thus, no exceedence of the ADI is expected from consumption of one portion of farmed Atlantic salmon fillet daily with regards to EQDM exposure. Nevertheless, with approximately 61% contribution to the ADI, farmed Atlantic salmon represents a major source of dietary EQDM exposure. Since EQ may also be present in feed for terrestrial farmed animals, the contribution of EQ and EQDM from all relevant food sources warrants further investigation.

5. Conclusions

Taken together, the results obtained in the present study indicate that subchronic dietary exposure to EQDM at levels above 10 mg/kg body weight/day disrupts hepatic lipid metabolism through impairment of fatty acid β-oxidation, leading to increased lipid deposition and steatosis in male BALB/c mice. Moreover, upstream analysis of hepatic proteome profiles revealed that EQDM-induced hepatotoxicity is likely mediated through activation of the orphan nuclear receptors PXR and/or CAR as well as induction of a NRF2-mediated oxidative stress response.

An ADI of 0.006 mg EQDM/kg body weight was derived from the benchmarch dose modelling of data obtained in the present study.

Role of the funding source

The sponsors of the present study approved the study design developed by the authors. The sponsors had no involvement in the collection, the analysis or interpretation of data, or in the writing of the manuscript.

Submission declaration

This manuscript has not been published previously and is not under consideration for publication elsewhere. The publication of the present article is approved by all authors and by the responsible authorities where the work was carried out. If accepted, the article will not be published elsewhere including electronically in the same form, in English or any other language, without the written consent of the copyright holder.

Acknowledgements

This study was financed by the Norwegian Seafood Research Fund (FHF), the Marine Ingredients Organisation (IFFO), Marine Harvest ASA, EWOS AS/Cargill Aqua Nutrition, Biomar AS, Skretting AS and Europharma (FHF project no. 901327). The authors wish to thank the technical staff at the Institute of Marine Research for assistance with animal care, sample preparation and analyses.

Appendix A. Supplementary data

Supplementary data related to this article can be found at http://dx.doi.org/10.1016/j.fct.2018.06.005.

Transparency document

Transparency document related to this article can be found online at http://dx.doi.org/10.1016/j.fct.2018.06.005.

References

Augustyniak, A., Niezgoda, A., Skolimowski, J., Kontek, R., Błaszczyk, A., 2012. Cytotoxicity and genotoxicity of ethoxyquin dimers. Bromatol. Chem. Toksykol. 45, 228–234.

Begriche, K., Igoudjil, A., Pessayre, D., Fromenty, B., 2006. Mitochondrial dysfunction in NASH: causes, consequences and possible means to prevent it. Mitochondrion 6 (1), 1–28.

Begriche, K., Massart, J., Robin, M.-A., Borgne-Sanchez, A., Fromenty, B., 2011. Drug-induced toxicity on mitochondria and lipid metabolism: mechanistic diversity and deleterious consequences for the liver. J. Hepatol. 54 (4), 773–794.

Bohne, V.J.B., Hove, H., Hamre, K., 2007a. Simultaneous quantitative determination of the synthetic antioxidant ethoxyquin and its major metabolite in Atlantic salmon (Salmo Salar, L), ethoxyquin dimer, by reversed-phase high-performance liquid chromatography with fluorescence detection. J. AOAC Int. 90 (2), 587–597.

Bohne, V.J.B., Hamre, K., Arukwe, A., 2007b. Hepatic metabolism, phase I and II biotransformation enzymes in Atlantic salmon (Salmo Salar, L) during a 12 Week feeding period with graded levels of the synthetic antioxidant, ethoxyquin. Food Chem. Toxicol. 45 (5), 733–746.

Bohne, V.J.B., Lundebye, A.-K., Hamre, K., 2008. Accumulation and depuration of the synthetic antioxidant ethoxyquin in the muscle of Atlantic salmon (Salmo Salar L.). Food Chem. Toxicol.: Int. J. Publ. British Indust. Biol. Res. Assoc. 46 (5), 1834–1843.

Błaszczyk, A., Augustyniak, A., Skolimowski, J., 2013. Ethoxyquin: an antioxidant used in animal feed. Int. J. Food Sci. 2013, 585931 12 pages.

Charles River Technical Resources: BALB/c Mouse, Clinical Pathology Data for BALB/c Mouse Colonies in North America for January 2008–December 2012. http://www.criver.com/files/pdfs/rms/balbc/rm_rm_r_balb-c_mouse_clinical_pathology_data.aspx. (Accessed 13 October 2017).

Cox, J., Mann, M., 2008. MaxQuant enables high peptide identification rates, individualized ppb-range mass accuracies and proteome-wide protein quantification. Nat. Biotechnol. 26 (12), 1367–1372.

Cox, J., Neuhauser, N., Michalski, A., Scheltema, R.A., Olsen, J.V., Mann, M., 2011. Andromeda: a peptide search engine integrated into the MaxQuant environment. J. Proteome Res. 10 (4), 1794–1805.

Cox, J., Hein, M.Y., Luber, C.A., Paron, I., Nagaraj, N., Mann, M., 2014. Accurate proteome-wide label-free quantification by delayed normalization and maximal peptide ratio extraction, termed MaxLFQ. Mol. Cell. Proteomics 13 (9), 2513–2526.

de Koning, A.J., 2002. The antioxidant ethoxyquin and its analogues: a review. Int. J. Food Prop. 5 (2), 451–461.

European Food Safety Authority (EFSA), 2012. Scientific opinion: guidance on selected default values to be used by the EFSA scientific committee, scientific panels and units in the absence of actual measured data. EFSA J 10 (3), 2579–2610. https://doi.org/10.2903/j.efsa.2012.2579.

European Food Safety Authority, 2013. Reasoned opinion on the review of the existing maximum residue levels (MRLs) for ethoxyquin according to article 12 of regulation (EC) No 396/2005. EFSA J. 11 (5). http://dx.doi.org/10.2903/j.efsa.2013.3231.

European Food Safety Authority (EFSA), 2017. Update: use of the benchmark dose approach in risk assessment. EFSA J. 15 (1). http://dx.doi.org/10.2903/j.efsa.2017.4658.

Fromenty, B., Pessayre, D., 1995. Inhibition of mitochondrial beta-oxidation as a mechanism of hepatotoxicity. Pharmacol. Therapeut. 67 (1), 101–154.

Fromenty, B., Pessayre, D., 1997. Impaired mitochondrial function in microvesicular steatosis. Effects of drugs, ethanol, hormones and cytokines. J. Hepatol. 26 (Suppl. 2), 43–53.
Gao, J., Xie, W., 2010. Pregnane X receptor and constitutive androstane receptor at the crossroads of drug metabolism and energy metabolism. Drug Metabol. Dispos.: Biological Fate Chem. 38 (12), 2091–2095.
Gu, X., Manautou, J.E., 2012. Molecular Mechanisms Underlying Chemical Liver Injury. Expert Rev. Mol. Med. 14, e4.
Guengerich, F.P., 2006. Cytochrome P450s and other enzymes in drug metabolism and toxicity. AAPS J. 8 (1), E101–E111.
Gupta, P.K., Boobis, A., 2005. Ethoxyquin (Addendum). http://www.inchem.org/documents/jmpr/jmpmono/v2005pr10.pdf.
Hamre, K., Næss, T., Espe, M., Holm, J.C., Lie, Ø, 2001. A formulated diet for Atlantic halibut (Hippoglossus Hippoglossus, L.) Larvae. Aquacult. Nutr. 7 (2), 123–132.
Hayes, J.D., Chanas, S.A., Henderson, C.J., McMahon, M., Sun, C., Moffat, G.J., Wolf, C.R., Yamamoto, M., 2000. "The Nrf2 transcription factor contributes both to the basal expression of glutathione S-Transferases in mouse liver and to their induction by the chemopreventive synthetic antioxidants, butylated hydroxyanisole and ethoxyquin. Biochem. Soc. Trans. 28 (2), 33–41.
He, P., Ackman, R.G., 2000. Residues of ethoxyquin and ethoxyquin dimer in ocean-farmed salmonids determined by high-pressure liquid chromatography. J. Food Sci. 65 (8), 1312–1314.
Hernández, M.E., Reyes, J.L., Gómez-Lojero, C., Sayavedra, M.S., Meléndez, E., 1993. Inhibition of the renal uptake of P-Aminohippurate and tetraethylammonium by the antioxidant ethoxyquin in the rat. Food Chem. Toxicol. 31 (5), 363–367.
Hobson-Frohock, A., 1982. Residues of ethoxyquin in poultry tissues and eggs. J. Sci. Food Agric. 33 (12), 1269–1274.
Jaeschke, H., Gores, G.J., Cederbaum, A.I., Hinson, J.A., Pessayre, D., Lemasters, J.J., 2002. Mechanisms of hepatotoxicity. Toxicol. Sci.: Off. J. Soc. Toxicol. 65 (2), 166–176.
JMPR, 1998. Ethoxyquin. JMPR Evaluations. http://www.inchem.org/documents/jmpr/jmpmono/v098pr09.htm.
Kahl, R., Netter, K.J., 1977. Ethoxyquin as an inducer and inhibitor of phenobarbital-type cytochrome P-450 in rat liver microsomes. Toxicol. Appl. Pharmacol. 40 (3), 473–483.
Kensler, T.W., Wakabayashi, N., 2010. Nrf2: Friend or Foe for Chemoprevention? Carcinogenesis 31 (1), 90–99.
Kim, H.L., 1991. Accumulation of ethoxyquin in the tissue. J. Toxicol. Environ. Health 33 (2), 229–236.
Klotz, L.-O., Steinbrenner, H., October 2017. Cellular adaptation to xenobiotics: interplay between xenosensors, reactive oxygen species and FOXO transcription factors. Redox Biol. 13, 646–654.
Lalwani, N.D., Reddy, M.K., Qureshi, S.A., Moehle, C.M., Hayashi, H., Reddy, J.K., 1983. "Noninhibitory effect of antioxidants ethoxyquin, 2(3)-tert-butyl-4-hydroxyanisole and 3,5-di-tert-butyl-4-hydroxytoluene on hepatic peroxisome proliferation and peroxisomal fatty acid β-oxidation induced by a hypolipidemic agent in rats. Canc. Res. 43 (4), 1680–1687.
Lie, Ø., Sandvin, A., Waagbø, R., 1994. Transport of alpha-tocopherol in Atlantic salmon (Salmo Salar) during vitellogenesis. Fish Physiol. Biochem. 13 (3), 241–247.
Lundebye, A.-K., Hove, H., Måge, A., Bohne, V.J.B., Hamre, K., 2010. Levels of synthetic antioxidants (ethoxyquin, butylated hydroxytoluene and butylated hydroxyanisole) in fish feed and commercially farmed fish. Food Addit. Contam. Part A Chem. Anal. Control Expo. Risk Assess. 27 (12), 1652–1657.
Magrane, M., UniProt Consortium, 2011. UniProt Knowledgebase: a hub of integrated protein data, *Database*. 2011, bar009. https://doi.org/10.1093/database/bar009.
Ørnsrud, R., Arukwe, A., Bohne, V., Pavlikova, N., Lundebye, A.-K., 2011. Investigations on the metabolism and potentially adverse effects of ethoxyquin dimer, a major metabolite of the synthetic antioxidant ethoxyquin in salmon muscle. J. Food Protect. 74 (9), 1574–1580.
Patel, V., Sanyal, A.J., 2013. Drug-induced steatohepatitis. Clin. Liver Dis. 17 (4), 533–546 vii.
Pessayre, D., Mansouri, A., Berson, A., Fromenty, B., 2010. Mitochondrial involvement in drug-induced liver injury. Handb. Exp. Pharmacol. 196, 311–365.
Pessayre, D., Fromenty, B., Berson, A., Robin, M.-A., Lettéron, P., Moreau, R., Mansouri, A., 2012. Central role of mitochondria in drug-induced liver injury. Drug Metabol. Rev. 44 (1), 34–87.
R Core Team, 2017. R: a Language and Environment for Statistical Computing. R Foundation for Statistical Computing, Vienna, Austria. https://www.R-project.org/.
Rao, M.S., Reddy, J.K., 2001. Peroxisomal beta-oxidation and steatohepatitis. Semin. Liver Dis. 21 (1), 43–55.
Rao, M.S., Lalwani, N.D., Watanabe, T.K., Reddy, J.K., 1984. Inhibitory effect of anti-oxidants ethoxyquin and 2(3)-tert-butyl-4-hydroxyanisole on hepatic tumorigenesis in rats fed ciprofibrate, a peroxisome proliferator. Canc. Res. 44 (3), 1072–1076.
Rasinger, J.D., Carroll, T.S., Lundebye, A.-K., Hogstrand, C., 2014. Cross-omics gene and protein expression profiling in juvenile female mice highlights disruption of calcium and zinc signalling in the brain following dietary exposure to CB-153, BDE-47, HBCD or TCDD. Toxicology 321 (0), 1–12.
Reyes, J., Hernández, M.E., Meléndez, E., Gómez-Lojero, C., 1995. Inhibitory effect of the antioxidant ethoxyquin on electron transport in the mitochondrial respiratory chain. Biochem. Pharmacol. 49 (3), 283–289.
Schumacher, J.D., Guo, G.L., 2015. Mechanistic review of drug-induced steatohepatitis. Toxicol. Appl. Pharmacol. 289 (1), 40–47.
Shen, G., Kong, A.-N., 2009. Nrf2 plays an important role in coordinated regulation of phase II drug metabolism enzymes and phase III drug transporters. Biopharm. Drug Dispos. 30 (7), 345–355.
Skaare, J.U., Roald, S.O., 1977. Ethoxyquin (EMQ) residues in Atlantic salmon measured by fluorimetry and gas chromatography (GLC). Nord. Veterinaermed. 29 (4–5), 232–236.
Staudinger, J.L., Goodwin, B., Jones, S.A., Hawkins-Brown, D., MacKenzie, K.I., LaTour, A., Liu, Y., 2001. The nuclear receptor PXR is a lithocholic acid sensor that protects against liver toxicity. Proc. Natl. Acad. Sci. U.S.A. 98 (6), 3369–3374.
Tastesen, H.S., Keenan, A.H., Madsen, L., Kristiansen, K., Liaset, B., 2014. Scallop protein with endogenous high taurine and glycine content prevents high-fat, high-sucrose-induced obesity and improves plasma lipid profile in male C57BL/6J mice. Amino Acids 46 (7), 1659–1671.
Torstensen, B.E., Espe, M., Stubhaug, I., Lie, Ø., 2011. Dietary plant proteins and vegetable oil blends increase adiposity and plasma lipids in atlantic salmon (Salmo Salar L.). Br. J. Nutr. 106 (5), 633–647.
Tyanova, S., Temu, T., Cox, J., 2016. The MaxQuant computational platform for mass spectrometry-based shotgun proteomics. Nat. Protoc. 11 (12), 2301–2319.
Wada, T., Gao, J., Xie, W., 2009. PXR and CAR in energy metabolism. Trends Endocrinol. Metabol. 20 (6), 273–279.
Wang, J., Ai, Q., Mai, K., Xu, H., Zuo, R., Xu, W., Zhang, W., Zhang, C., 2015. Effects of dietary ethoxyquin on growth, feed Utilization and residue in the muscle of juvenile Japanese seabass, lateolabrax japonicus. Aquacult. Res. 46 (11), 2656–2664.
Wheeler, M., Bailer, J., 2008. Model averaging software for dichotomous dose response risk estimation. J. Stat. Software 26 (5), 1–15.
Wiśniewski, J.R., Zougman, A., Nagaraj, N., Mann, M., 2009. Universal sample preparation method for proteome analysis. Nat. Methods 6 (5), 359–362.
Xie, W., Barwick, J.L., Downes, M., Blumberg, B., Simon, C.M., Nelson, M.C., Neuschwander-Tetri, B.A., Brunt, E.M., Guzelian, P.S., Evans, R.M., 2000. Humanized xenobiotic response in mice expressing nuclear receptor SXR. Nature 406 (6794), 435–439.
Zhou, J., Zhai, Y., Mu, Y., Gong, H., Uppal, H., Toma, D., Ren, S., Evans, R.M., Wen Xie, W., 2006. A novel pregnane X receptor-mediated and sterol regulatory element-binding protein-independent lipogenic pathway. J. Biol. Chem. 281 (21), 15013–15020.